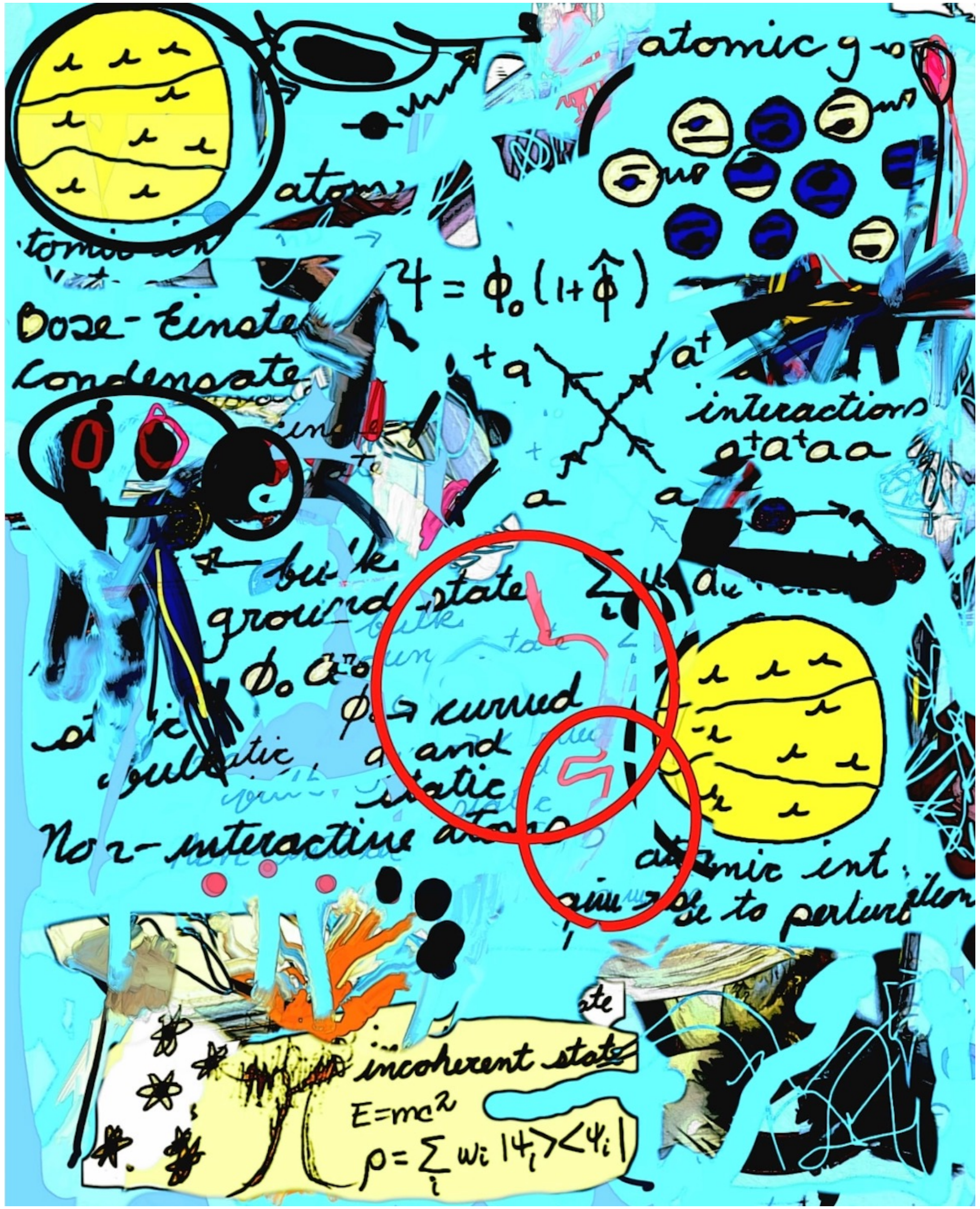

Quantum information and quantum metrology for Fundamental Physics

Ivette Fuentes
University of Southampton
Keble College, Oxford

University of Southampton

Keble College

BEC in spacetime

A covariant formalism is available

Phonons are a relativistic quantum field

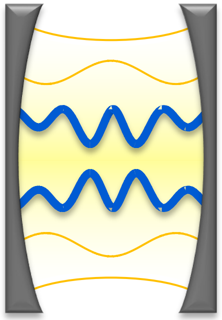

$$\mathcal{L} = -\sqrt{-g}\left\{ g^{\mu\nu}\partial_\mu \hat{\Phi}^\dagger \partial_\nu \hat{\Phi} + \left(\frac{m^2c^2}{\hbar^2} + V\right)\hat{\Phi}^\dagger\hat{\Phi} + U\left(\hat{\Phi}^\dagger\hat{\Phi}, \lambda_i\right)\right\}$$

$$U\left(\hat{\Phi}^\dagger\hat{\Phi}, \lambda_i\right) \approx \frac{\lambda}{2}\hat{\Phi}^\dagger\hat{\Phi}^\dagger\hat{\Phi}\hat{\Phi}$$

$$\widehat{\Phi} = \phi(1+\widehat{\psi})$$

For uniform density

$$\Box\psi = \frac{1}{\sqrt{-\mathfrak{g}}}\partial_\mu(\sqrt{-\mathfrak{g}}\,\mathfrak{g}^{\mu\nu}\partial_\mu)\psi$$

effective metric

$$\mathfrak{g}_{ab} = \rho\frac{c}{c_s}\left[g_{ab} + \left(1 - \frac{c_s^2}{c^2}v_a v_b\right)\right]$$

spacetime metric

analogue metric

Demonstrate QFT in CS

Fagnocchi et. al NJP 2010 (quantum field flat spacetime)
Visser & Molina-Paris NJP 2010 (classical field in curved spacetime)
D. E. Bruschi et. al., NJP 16 5:053041, 2014 (quantum field in curved spatime)
D. Hartley. et. al., PRD 89 025011, 2018

Analogue spacetimes and simulations

Analogue Systems

moving fluid
superfluid helium
Bose–Einstein condensate
gravity waves in water
electromagnetic waves in a dielectric medium

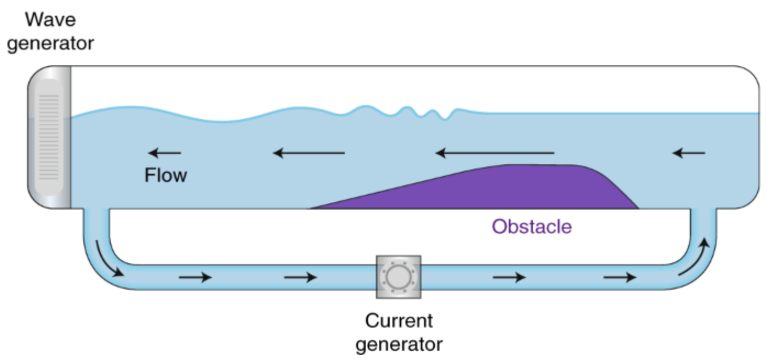

Published: 12 October 2014

Observation of self-amplifying Hawking radiation in an analogue black-hole laser

Jeff Steinhauer

Nature Physics **10**, 864–869 (2014) | Cite this article

13k Accesses | **227** Citations | **388** Altmetric | Metrics

Published: 12 June 2017

Rotational superradiant scattering in a vortex flow

Theo Torres, Sam Patrick, Antonin Coutant, Maurício Richartz, Edmund W. Tedford & Silke Weinfurtner

Nature Physics **13**, 833–836 (2017) | Cite this article

11k Accesses | **141** Citations | **240** Altmetric | Metrics

Quantum analogue of a Kerr black hole and the Penrose effect in a Bose-Einstein condensate

D. D. Solnyshkov, C. Leblanc, S. V. Koniakhin, O. Bleu, and G. Malpuech
Phys. Rev. B **99**, 214511 – Published 24 June 2019

PHYSICAL REVIEW D
covering particles, fields, gravitation, and cosmology

Highlights Recent Accepted Collections Authors Referees Search Press About

Hawking temperature and phonon emission in acoustic holes

Massimo Mannarelli, Dario Grasso, Silvia Trabucco, and Maria Luisa Chiofalo
Phys. Rev. D **103**, 076001 – Published 2 April 2021

Covariant formulation

$$\mathcal{L} = -\sqrt{-g}\left\{g^{\mu\nu}\partial_\mu\hat{\Phi}^\dagger\partial_\nu\hat{\Phi} + \left(\frac{m^2c^2}{\hbar^2} + V\right)\hat{\Phi}^\dagger\hat{\Phi} + U\left(\hat{\Phi}^\dagger\hat{\Phi}, \lambda_i\right)\right\}$$

BEC: barotropic, irrotational and inviscid fluid, in a covariant formalism.

i) simulating a spacetime metric
ii) simulating the effects of spacetime dynamics on a phononic field.

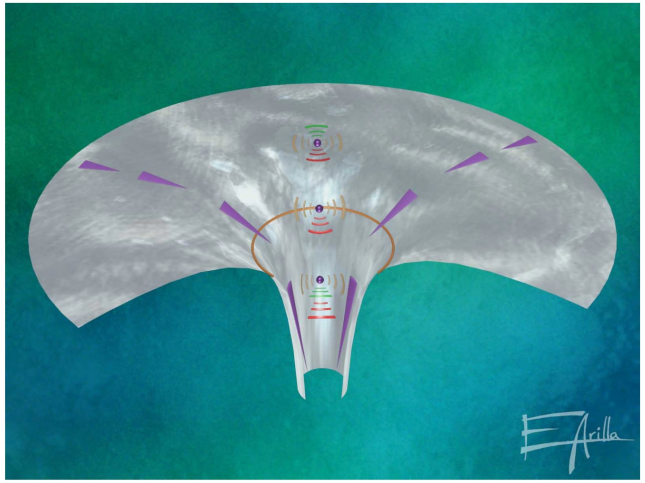

1. Superfluid regime (barotropic and inviscid)

Bogoliubov approximation so $\left\langle\hat{\Phi}\right\rangle \approx \phi$ and $\left\langle\hat{\psi}^\dagger\hat{\psi}\right\rangle \ll |\phi|^2$.

$$\hat{\Phi} = \phi\left(1+\hat{\psi}\right) \qquad \phi = \sqrt{\rho}e^{i\theta}$$

2. In the long wavelength regime $|k| \ll \frac{\sqrt{2}}{\xi}\left(1+\frac{\hbar^2}{2m^2\xi^2u_0^2}\right)\min\left[1, \frac{mu_0\xi}{\sqrt{2}\hbar}\right],$

Velocity flows $u_\mu = \frac{\hbar}{m}\partial_\mu\theta$

Scattering length

Healing length $\xi = \frac{1}{\sqrt{\lambda\rho}}.$

$\lambda = 8\pi a.$

phonons should have wavelengths far longer than the healing length

$U\left(\phi^\dagger\phi, \lambda\right) = \frac{1}{2}\lambda\left|\phi^\dagger\phi\right|^2 + \cdots$

Strength of the interaction

The fluctuations are massless phonons

Plugging the Bogoliubov approximation in the equations of motion for the Lagrangian yields

$$\frac{1}{\sqrt{-G}}\partial_\mu\sqrt{-G}G^{\mu\nu}\partial_\nu\hat{\psi} = 0$$

$v^\mu = \frac{c}{|u|}u^\mu$ Normalized velocity flows

$$G_{\mu\nu} = \frac{\rho c}{c_s}\left[g_{\mu\nu} + \left(1-\frac{c_s^2}{c^2}\right)\frac{v_\mu v_\nu}{c^2}\right].$$

Effective speed of sound

$c_s^2 = \frac{c^2c_0^2}{c_0^2+|u|^2}$

$c_0^2 = \frac{\hbar^2}{2m^2}\rho\partial_\rho^2U\left(\rho,\lambda\right) = \frac{\hbar^2}{2m^2}\lambda\rho.$

The equations of motion of the mean field ϕ can be split into real and imaginary components resulting in a continuity equation

$$\nabla_\mu \left(\rho u^\mu\right) = 0$$

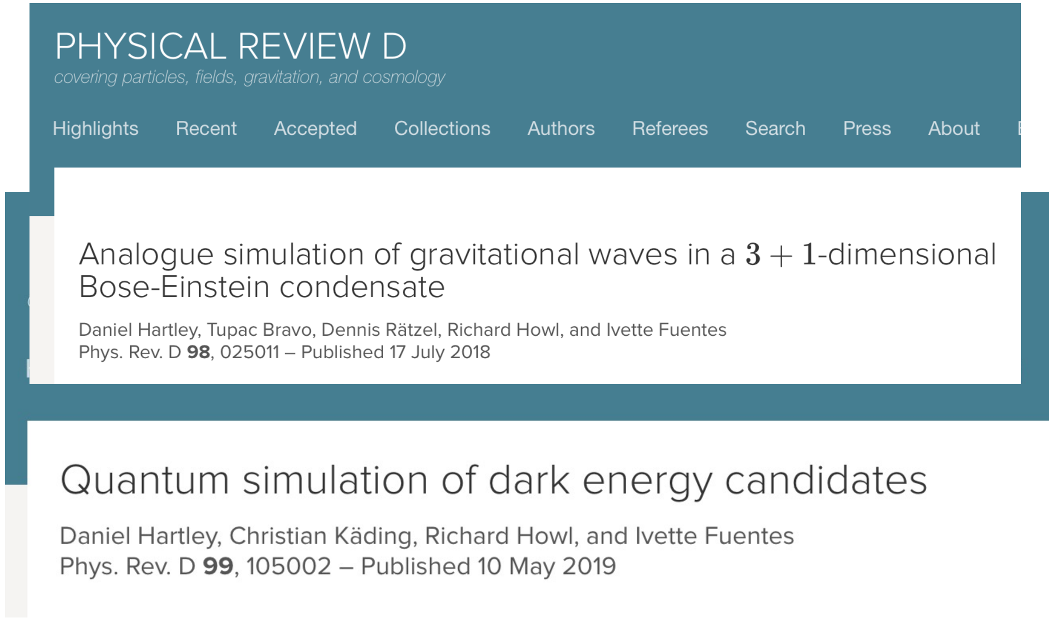
PHYSICAL REVIEW D
covering particles, fields, gravitation, and cosmology
Highlights Recent Accepted Collections Authors Referees Search Press About

Analogue simulation of gravitational waves in a $3+1$-dimensional Bose-Einstein condensate
Daniel Hartley, Tupac Bravo, Dennis Rätzel, Richard Howl, and Ivette Fuentes
Phys. Rev. D **98**, 025011 – Published 17 July 2018

Quantum simulation of dark energy candidates
Daniel Hartley, Christian Käding, Richard Howl, and Ivette Fuentes
Phys. Rev. D **99**, 105002 – Published 10 May 2019

and an equation directly relating bulk field properties with potentials:

$$|u|^2 = c^2 + \frac{\hbar^2}{m^2}\left\{V + \partial_\rho U\left(\rho,\lambda\right) - \frac{\nabla_\mu \nabla^\mu \sqrt{\rho}}{\sqrt{\rho}}\right\}.$$

$$G_{\mu\nu} \propto \begin{pmatrix} -\left(c_s^2 - v^2\right)/c^2 & -v_i/c \\ -v_j/c & \delta_{ij} \end{pmatrix}$$

Acoustic metric commonly used.
We can obtain it in our covariant formulation in the following way.

Flat spacetime

We define a “flat” acoustic metric for the phonons in the absence of any simulated fields as the acoustic metric in coordinates with the following conditions:

1. The background spacetime is flat, i.e. $g_{\mu\nu} = \eta_{\mu\nu} = \mathrm{diag}\,(-1, 1, 1, 1)$,
2. No flows, i.e. $v_i = 0$,
3. Static density, i.e. $\rho_0 = \rho_0\,(\boldsymbol{x}) \Leftrightarrow \partial_t \rho_0 = 0$, and
4. Unperturbed interaction strength λ, so $\partial_t \lambda = \partial_x \lambda = 0$.

The acoustic metric in $n+1$ dimensions then has the form

$$G^0_{\mu\nu} = \frac{\rho_0 c}{c_{s0}} \begin{pmatrix} -c_{s0}^2/c^2 & \\ & \mathbb{I}_n \end{pmatrix} \qquad c_{s0} = \frac{\hbar}{m}\sqrt{4\pi\rho\, a}.$$

Simplest simulation

Gravitational wave in 1+1 dimension

$$g_{\mu\nu} = \eta_{\mu\nu} + h_{\mu\nu}$$

A gravitational wave moving in the z-direction

$$\eta_{\mu\nu} = \begin{pmatrix} -c^2 & 0 & 0 & 0 \\ 0 & 1 & 0 & 0 \\ 0 & 0 & 1 & 0 \\ 0 & 0 & 0 & 1 \end{pmatrix}$$

$$h_{\mu\nu} = \begin{pmatrix} 0 & 0 & 0 & 0 \\ 0 & h_+(t) & h_\times(t) & 0 \\ 0 & h_\times(t) & -h_+(t) & 0 \\ 0 & 0 & 0 & 0 \end{pmatrix}$$

time-dependent perturbations in two different polarisations.

In one dimension

$$ds^2 = -c^2\, dt^2 + (1 + h_+(t))\, dx^2.$$

BEC in flat spacetime
in the absence of spatial flows

$v^t = c$ and $v^x = 0$, then the line element is conformal to:

$$ds^2 = -c_s^2\, dt^2 + dx^2$$

$$\mathfrak{g}_{ab} = \frac{\rho\, c_s}{c} \begin{pmatrix} -c_s^2 & 0 & 0 & 0 \\ 0 & 1 + h_+(t) & h_\times(t) & 0 \\ 0 & h_\times(t) & 1 - h_+(t) & 0 \\ 0 & 0 & 0 & 1 \end{pmatrix}$$

Research | Open Access | Published: 04 January 2015

Analog quantum simulation of gravitational waves in a Bose-Einstein condensate

Tupac Bravo, Carlos Sabín & Ivette Fuentes

EPJ Quantum Technology 2, Article number: 3 (2015) | Cite this article

Now, if we consider that the speed of sound can depend on t:

$$c_s(t) = c_{s0}\, f(t),$$

$$c_{s0} = \frac{\hbar}{m}\sqrt{4\pi\rho\, a}.$$

the corresponding line element is conformal to:

$$ds^2 = -c_{s0}^2\, dt^2 + \frac{1}{(f(t))^2}\, dx^2.$$

Therefore, if the speed of sound varies in time such that

$$f(t) = (1 - \frac{A_+ \sin\Omega\, t}{2}),$$

we find, up to the first order in A_+:

$$ds^2 = -c_{s0}^2\, dt^2 + (1 + A_+ \sin\Omega\, t)\, dx^2.$$

So the experimental task is to modulate the speed of sound as:

$$c_s(t) = c_{s0}(1 - \frac{A_+ \sin\Omega\, t}{2}).$$

Vary scattering length using magnetic fields

background scattering length

$$a = a_{bg}(1 - \frac{\omega}{B - B_0})$$

Feshbach resonances

Recent experiments

Open Access

Thermalization by a synthetic horizon

Lotte Mertens, Ali G. Moghaddam, Dmitry Chernyavsky, Corentin Morice, Jeroen van den Brink, and Jasper van Wezel

Phys. Rev. Research **4**, 043084 – Published 8 November 2022

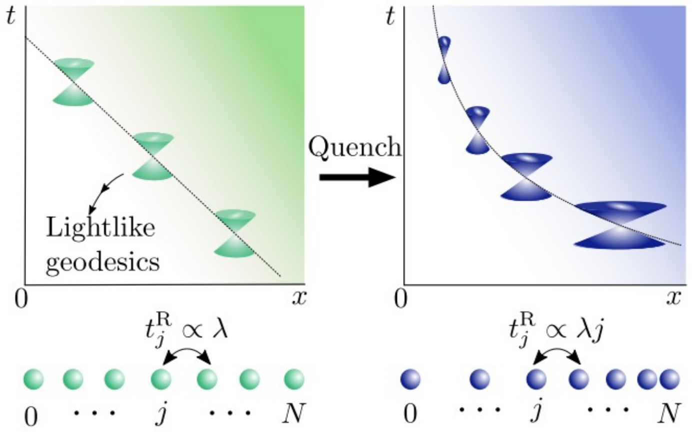

FIG. 1. Schematic overview of the quench set-up. In the top part of the figure a lightlike geodesic is drawn in a spacetime diagram for flat spacetime (left) and curved spacetime with a horizon at $x = 0$ (right). In the lower part the corresponding tight binding models are shown with constant hopping (left) and position dependent hopping (right).

28 November 2022 / Evrim Yazgin

Black hole simulation began glowing, providing hope for unifying gravity and quantum mechanics

The experiment may prove the existence of Hawking radiation.

Article | Published: 09 November 2022

Quantum field simulator for dynamics in curved spacetime

Celia Viermann, Marius Sparn, Nikolas Liebster, Maurus Hans, Elinor Kath, Álvaro Parra-López, Mireia Tolosa-Simeón, Natalia Sánchez-Kuntz, Tobias Haas, Helmut Strobel, Stefan Floerchinger & Markus K. Oberthaler

Nature **611**, 260–264 (2022) | Cite this article

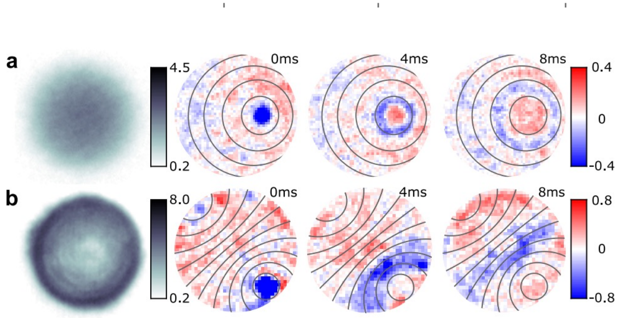

FIG. 2. **Configurable density distribution for hyperbolic and spherical geometry. a)** Density distribution of the condensate for hyperbolic geometry and expansion of a phononic wave packet depicted in th sate (blue under-, rec two-by-two region of p els. **b)** Density distrib the two-dimensional co propagation of the wav ing confirming the suc positive curvature. E the initial perturbatio respectively.

RESEARCH ARTICLE | PHYSICS

Experimental observation of curved light-cones in a quantum field simulator

Mohammadamin Tajik, Marek Gluza, Nicolas Sebe, +9, and Jörg Schmiedmayer Authors Info & Affiliations

Edited by Angel Rubio, Max-Planck-Institut fur Struktur und Dynamik der Materie, Hamburg, Germany; received January 23, 2023; accepted March 24, 2023

May 15, 2023 | 120 (21) e2301287120 | https://doi.org/10.1073/pnas.2301287120

Uses and Limitations

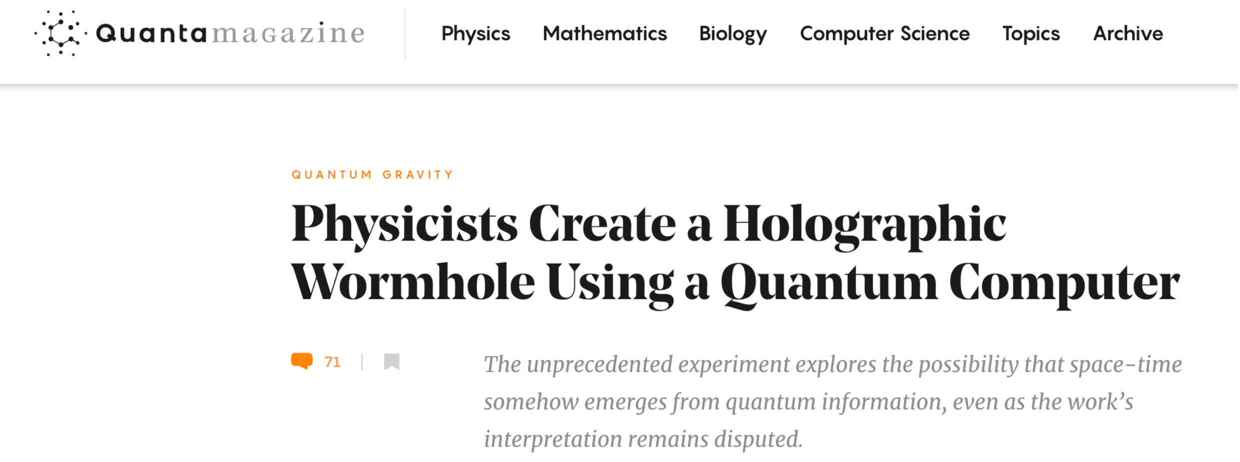
Quantamagazine | Physics | Mathematics | Biology | Computer Science | Topics | Archive

QUANTUM GRAVITY

Physicists Create a Holographic Wormhole Using a Quantum Computer

71

The unprecedented experiment explores the possibility that space-time somehow emerges from quantum information, even as the work's interpretation remains disputed.

-self-consistency checks
-useful to study the behaviour of matter under the influence of fields with non-linear behaviour since their non-linearities can make computer simulations challenging.

A good analogy can be an invaluable tool in studying a complex or inaccessible system but…

Analogue experiments can't falsify or verify a physical theory
(as much as a computer simulation can't do this either)

Attention!
New phenomena can be misinterpreted
Analogues cannot truly discover new effects

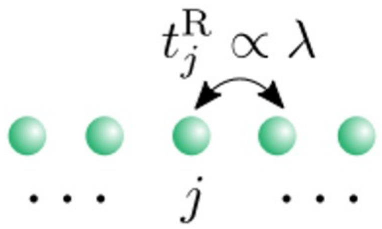

BEC in spacetime

A covariant formalism is available

Phonons are a relativistic quantum field

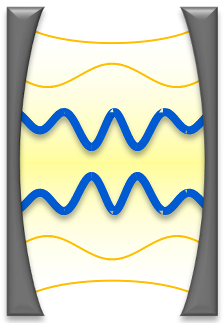

$$\mathcal{L} = -\sqrt{-g}\left\{g^{\mu\nu}\partial_\mu\hat{\Phi}^\dagger\partial_\nu\hat{\Phi} + \left(\frac{m^2c^2}{\hbar^2} + V\right)\hat{\Phi}^\dagger\hat{\Phi} + U\left(\hat{\Phi}^\dagger\hat{\Phi}, \lambda_i\right)\right\}$$

$$U\left(\hat{\Phi}^\dagger\hat{\Phi}, \lambda_i\right) \approx \frac{\lambda}{2}\hat{\Phi}^\dagger\hat{\Phi}^\dagger\hat{\Phi}\hat{\Phi}$$

$$\widehat{\Phi} = \phi(1 + \widehat{\psi})$$

For uniform density

$$\Box\,\psi = \frac{1}{\sqrt{-\mathfrak{g}}}\partial_\mu(\sqrt{-\mathfrak{g}}\mathfrak{g}^{\mu\nu}\partial_\mu)\psi$$

effective metric

$$\mathfrak{g}_{ab} = \rho\frac{c}{c_s}\left[g_{ab} + \left(1 - \frac{c_s^2}{c^2}v_a v_b\right)\right]$$

spacetime metric

analogue metric

Demonstrate QFT in CS

Fagnocchi et. al NJP 2010 (quantum field flat spacetime)

Visser & Molina-Paris NJP 2010 (classical field in curved spacetime)

D. E. Bruschi et. al., NJP 16 5:053041, 2014 (quantum field in curved spatime)

D. Hartley. et. al., PRD 89 025011, 2018

Atom interferometer: quantum spatial interferometery

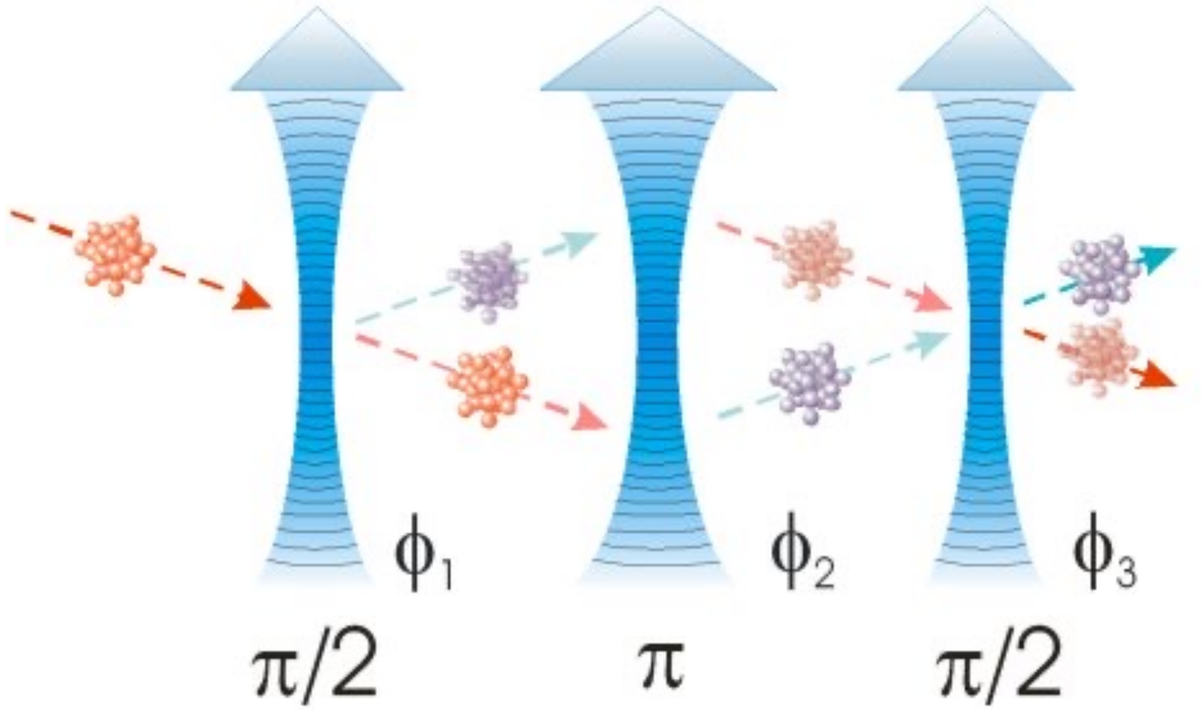

$$\delta a = 1 \Big/ \left(\sqrt{N} k T^2 \right)$$

Single particle detector, local

Interferometry in the <u>spatial domain</u>: limited by time of flight

Compatible with Newtonian physics

Gravimeters are going Big

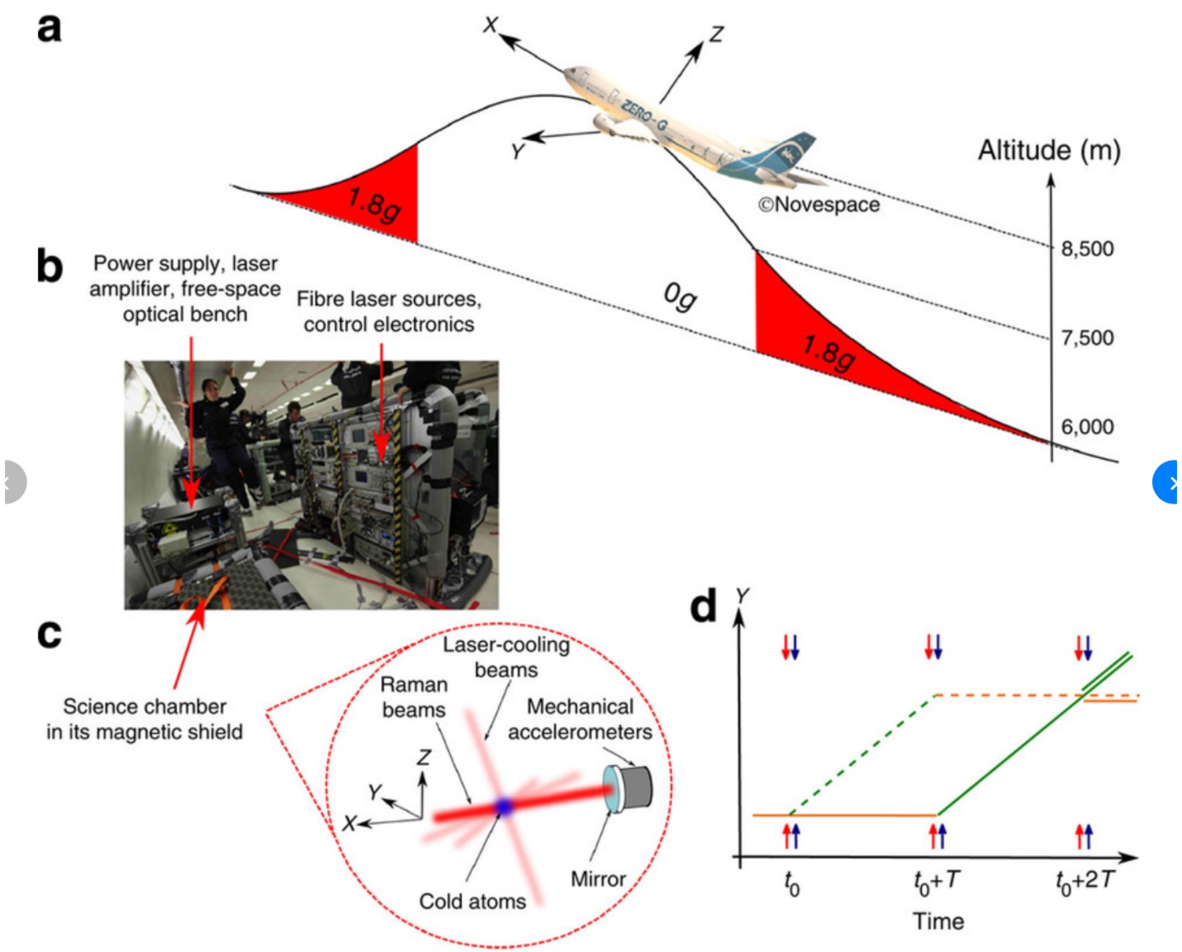

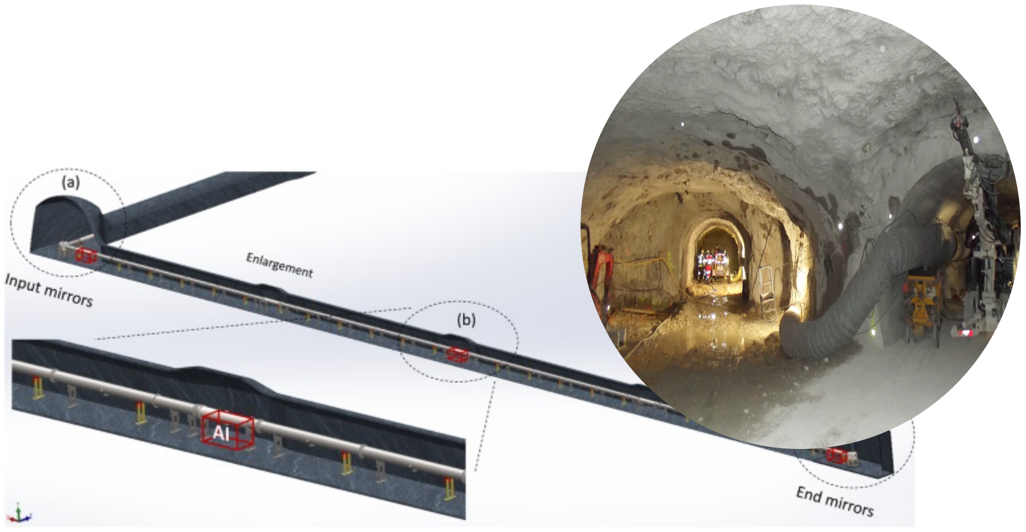

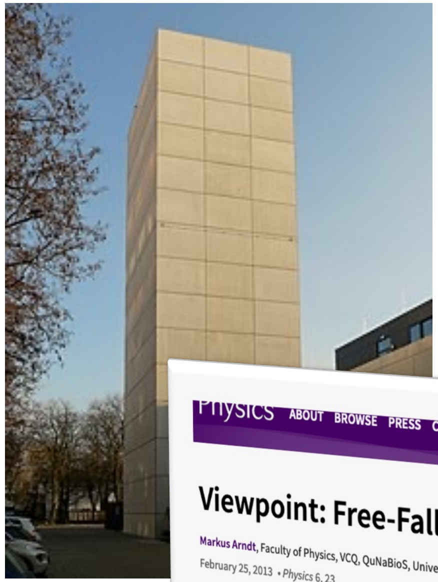

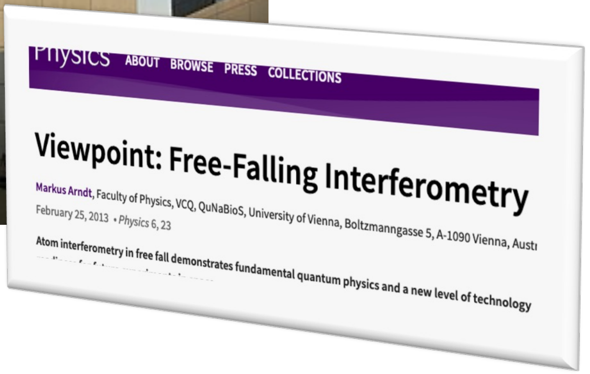
Physics ABOUT BROWSE PRESS COLLECTIONS

Viewpoint: Free-Falling Interferometry

Markus Arndt, Faculty of Physics, VCQ, QuNaBioS, University of Vienna, Boltzmanngasse 5, A-1090 Vienna, Austi

February 25, 2013 • Physics 6, 23

Atom interferometry in free fall demonstrates fundamental quantum physics and a new level of technology

But...I want one in my phone

Change of paradigm!

PHYSICAL REVIEW A
covering atomic, molecular, and optical physics and quantum information

Trapped-atom interferometer with ultracold Sr atoms

Xian Zhang, Ruben Pablo del Aguila, Tommaso Mazzoni, Nicola Poli, and Guglielmo M. Tino
Phys. Rev. A **94**, 043608 – Published 4 October 2016

Images

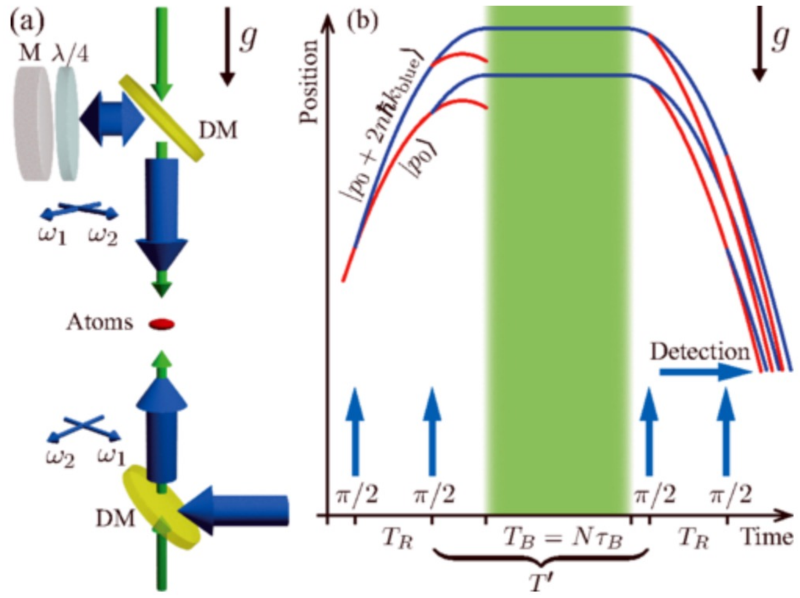

MINIATURIZED ATOM-CHIP GRAVIMETER

Matterwave interferometers based on cold atoms are commonly used as gravimeters. They reach accuracies of up to 10^{-9}g and are nowadays even commercially available.

We have demonstrated a compact quantum gravimeter, which employs an atom chip for the rapid and efficient creation of Bose-Einstein condensates (BEC). At the same time, the atom chip serves for complete state preparation of the atomic cloud and as a retroreflector for the laser beam to create an optical lattice. With the lattice, we split, redirect, and recombine the BEC to form a Mach-Zehnder interferometer and measure the local gravitational acceleration.

To extend the interferometer time and increase the device's sensitivity, we employ the optical lattice for an innovative launch mechanism. In this way, we acquire an intrinsic sensitivity of $\Delta g/g = 10^{-7}$, while keeping all atom-optical operations in a volume of less than a one-centimeter cube.

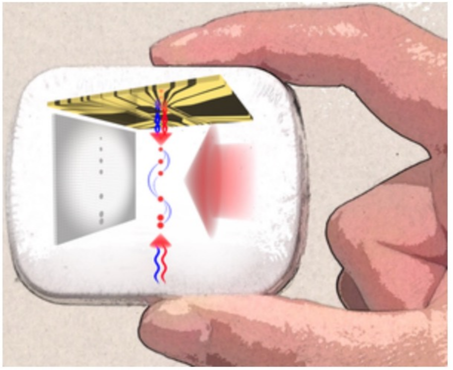

Image by S. Abend and E. Rasel/Leibniz Univ. of Hannover (Physics 9, 131, 2016)

RELATED PUBLICATIONS

S. Abend et. al. *Atom-Chip Fountain Gravimeter* Phys. Rev. Lett. **117**, 203003 (2016)

Quantum frequency interferometry

Howl & Fuentes arXiv:1902.09883

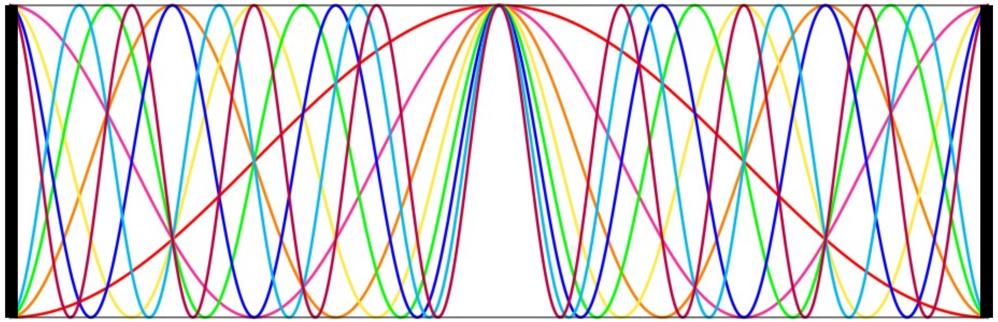

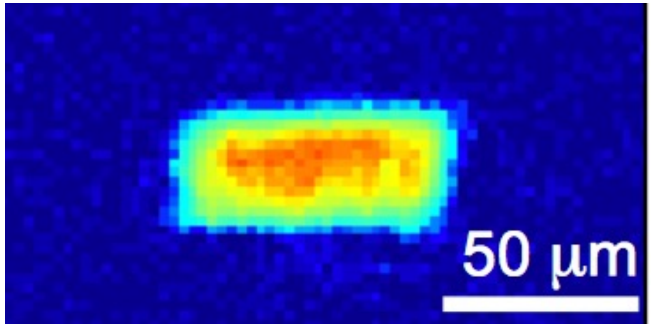

Uses interactions: collective excitations, entanglement between atoms

Implementation of frequency modes: phonons in a BEC (massless quantum field)

Interferometry in the frequency (time) domain, non-local

We use parametric amplification produced by the non-linearity introduced by atomic collisions

Compatible with General Relativity: underpinned by QFT in curved spacetime

BECs and quantum frequency interferometry

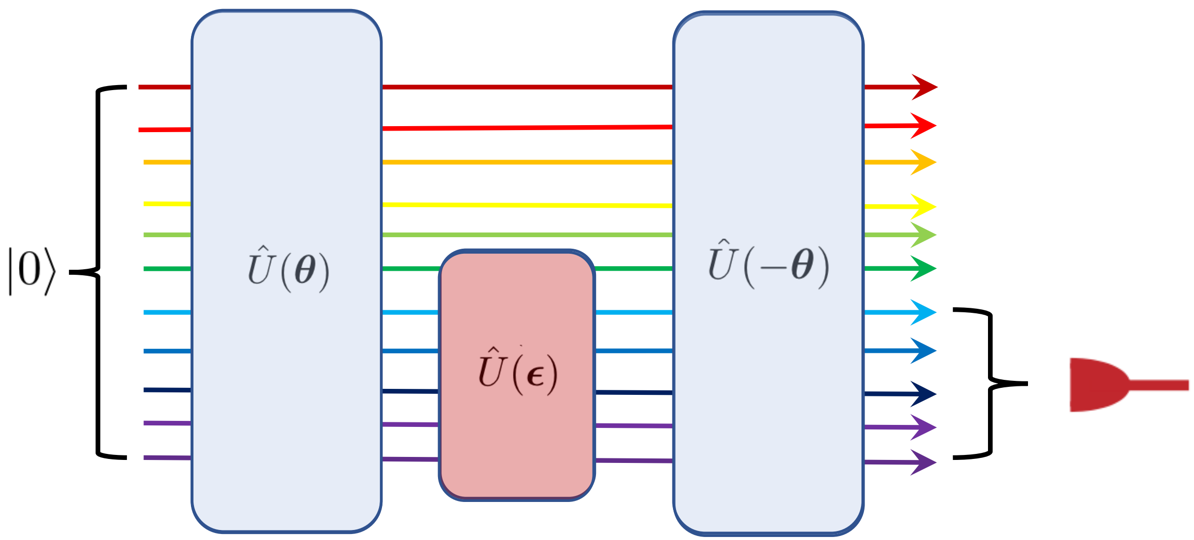

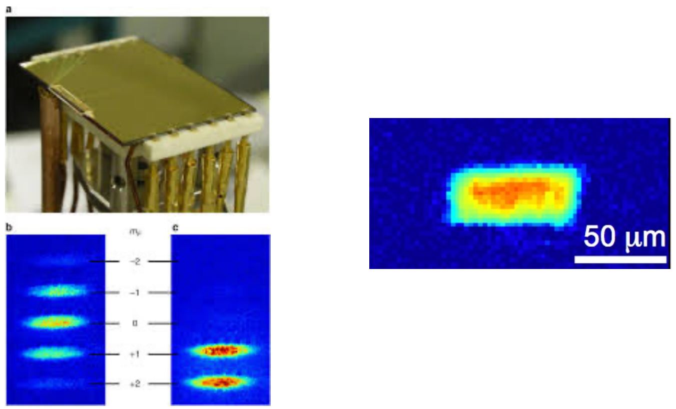

- Detector can be miniaturized
- High sensitivity
- High resilience to noise

Howl & Fuentes arXiv:1902.09883

Quantum sensors underpinned by QFTCS

- Continuous source gravitational wave detector
- Quantum relativistic clocks
- Dark energy
- Proper acceleration
- Local gravitational fields (UK patent No.1908538.0)
- Gravitational gradient (UK patent No. 2000112.9)
- Curvature
- Spacetime parameters
- Dark Matter!

Demonstrate particle creation by spacetime dynamics!

Bose Einstein Condensate in a box

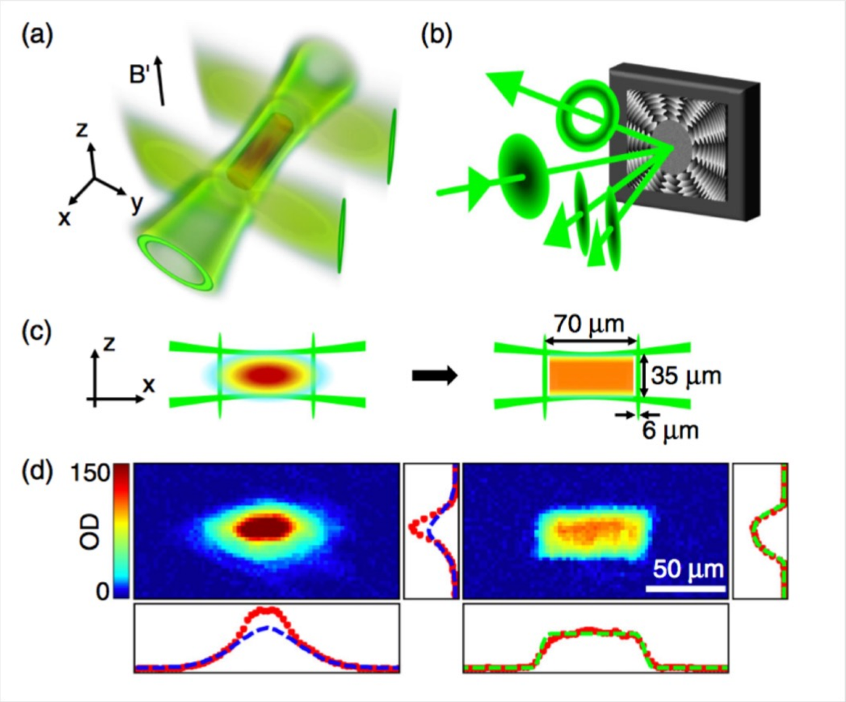

mean field (ground state)

$$\hat{\Phi} = \phi(1 + \widehat{\psi})$$

phonons
density fluctuations due to interactions

quasi-uniform density

$$\rho = \phi^{\dagger}\phi$$

Gaunt *et. al.* PRL 110 200406 (2013)

BEC in flat spacetime

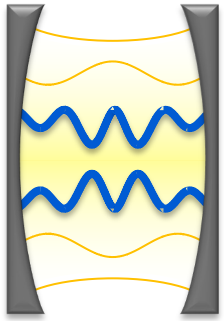

$$\mathfrak{g}_{ab} = \left(\frac{n_0^2\, c_s^{-1}}{\rho_0 + p_0}\right)\begin{pmatrix} -c_s^2 & 0 & 0 & 0 \\ 0 & 1 & 0 & 0 \\ 0 & 0 & 1 & 0 \\ 0 & 0 & 0 & 1 \end{pmatrix}$$

Minkowski space but with speed of sound

$$\tau = (c/c_s)t \;\Longrightarrow\; ds^2 = -cdt^2 + dx^2$$

phonons in a cavity-type 1-dimensional trap

$$\omega_n = \frac{n\,\pi\,c_s}{L}$$ spectrum

$$\Box\phi(t,x) = 0$$

$$\phi_n = \frac{1}{\sqrt{n\,\pi}} \sin\frac{n\pi(x - x_L)}{L}\, e^{-i\,\omega_n\,t}$$

Solutions to the K-G equation

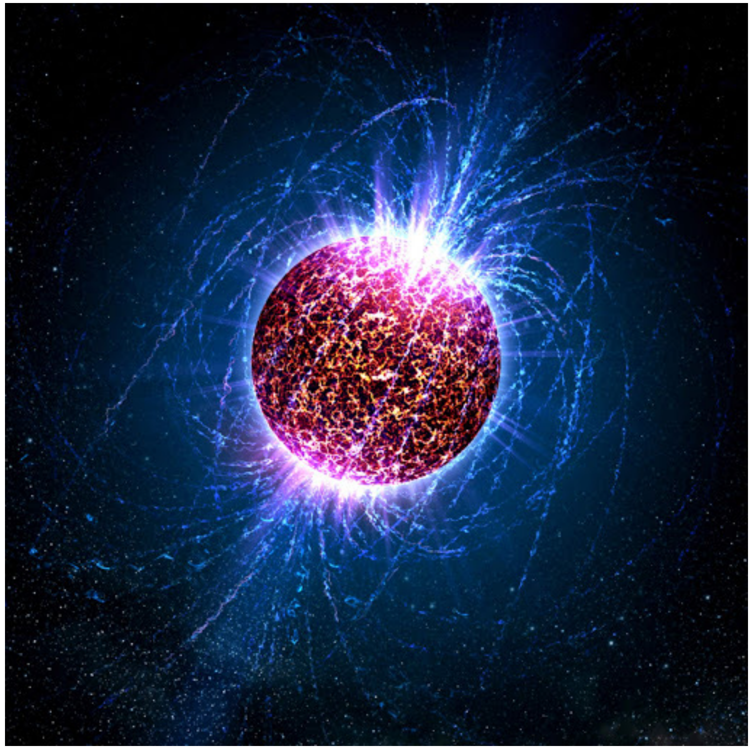

Gravitational wave spacetime

$$\mathfrak{g}_{ab} = \left(\frac{n_0^2\, c_s^{-1}}{\rho_0 + p_0}\right) \begin{pmatrix} -c_s^2 & 0 & 0 & 0 \\ 0 & 1 + h_+(t) & h_\times(t) & 0 \\ 0 & h_\times(t) & 1 - h_+(t) & 0 \\ 0 & 0 & 0 & 1 \end{pmatrix}$$

In a one-dimensional trap

$$ds^2 = -c_s^2\, dt^2 + (1 + h_+(t))\, dx^2.$$

$$h_+(t) = \epsilon \sin \Omega\, t$$

Continuous sources

$$\omega_n = \frac{n\, \pi\, c_s}{L}$$

Resonance!

$$g_{\mu\nu} = \eta_{\mu\nu} + h_{\mu\nu}$$

$$h_{\mu\nu} = \begin{pmatrix} 0 & 0 & 0 & 0 \\ 0 & h_+(t) & h_\times(t) & 0 \\ 0 & h_\times(t) & -h_+(t) & 0 \\ 0 & 0 & 0 & 0 \end{pmatrix}$$

Field transformations

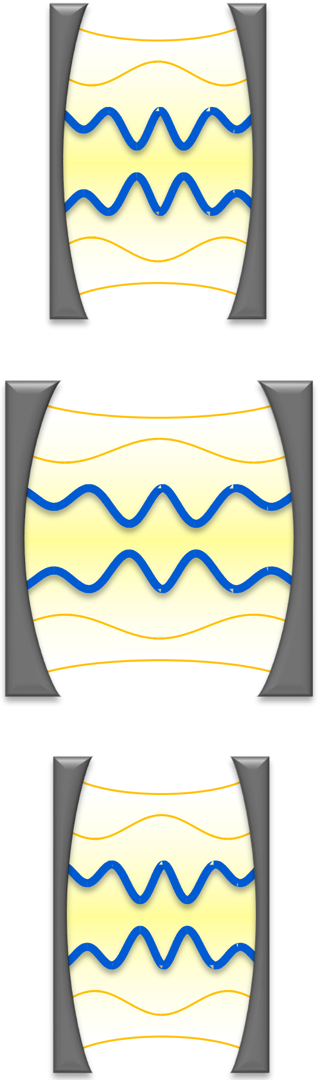

Bogoliubov transformations

$$\tilde{a}_m = \sum_n \left(\alpha_{mn}^* \, a_n - \beta_{mn}^* \, a_n^\dagger \right)$$

$$\alpha_{mn} = (\tilde{\phi}_m, \phi_n) \text{ and } \beta_{mn} = -(\tilde{\phi}_n, \phi_m^*)$$

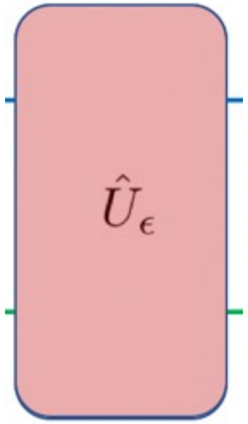

$$\begin{aligned} \beta_{jk}(t) &= -\frac{\epsilon}{2}\sqrt{\frac{n}{m}}\,\omega_m\, t\,[-x_L + (-1)^{m+n}(L + x_L)]\delta_{jm}\,\delta_{kn} + \mathcal{O}(\epsilon^2) \\ \alpha_{jk}(t) &= 0 + \mathcal{O}(\epsilon^2), \end{aligned}$$

Bruschi, Fuentes & Louko PRD (R) 2011

Field transformations

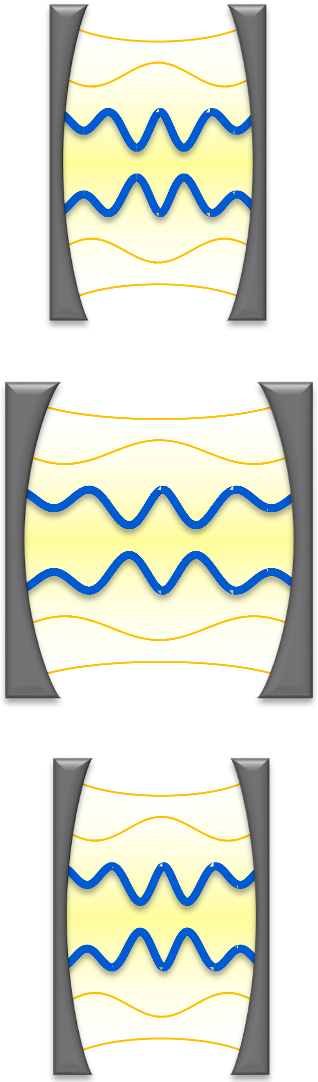

The dynamics of spacetime produces a Bogoliubov transformation on the field modes

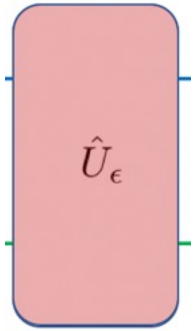

$$\tilde{a}_m = \sum_n \left(\alpha^*_{mn}\, a_n - \beta^*_{mn}\, a^\dagger_n \right)$$

$$\alpha_{mn} = (\tilde{\phi}_m, \phi_n) \text{ and } \beta_{mn} = -(\tilde{\phi}_n, \phi^*_m)$$

Bogoliubov transformation for monocromatic gravitational wave

$$\begin{aligned} \beta_{jk}(t) &= -\frac{\epsilon}{2}\sqrt{\frac{n}{m}}\,\omega_m\, t\,[-x_L + (-1)^{m+n}(L + x_L)]\delta_{jm}\,\delta_{kn} + \mathcal{O}(\epsilon^2) \\ \alpha_{jk}(t) &= 0 + \mathcal{O}(\epsilon^2), \end{aligned}$$

Application: gravitational wave detector

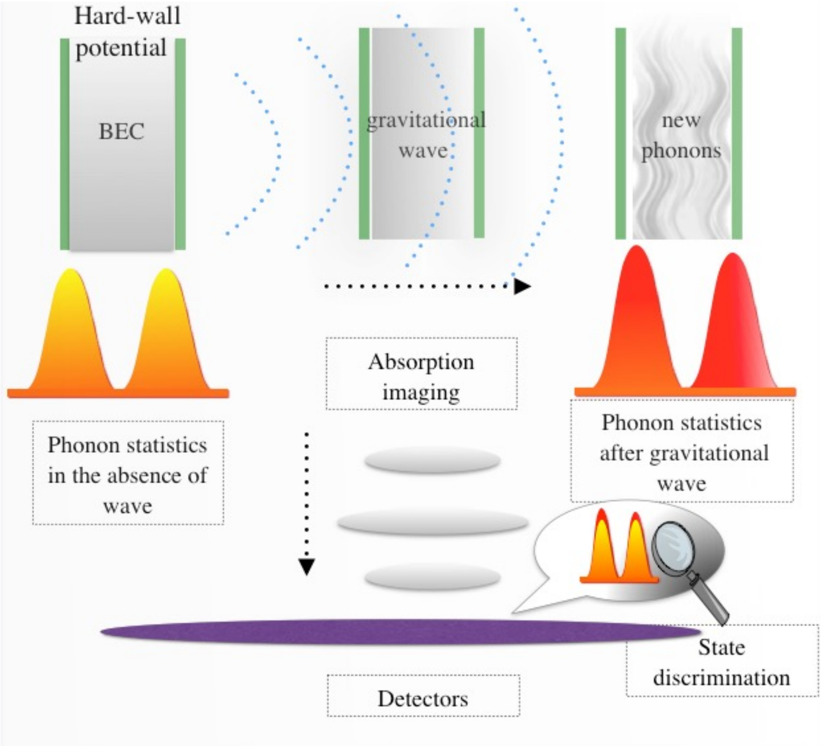

Phonon creation by gravitational waves

Carlos Sabín[1], David Edward Bruschi[2], Mehdi Ahmadi[1] and Ivette Fuentes[1]

Published 7 August 2014 •

New Journal of Physics, Volume 16, August 2014

Requires high phonon numbers ~$\sqrt{N_0}$
and long phonon lifetimes ~10s

Three mode application

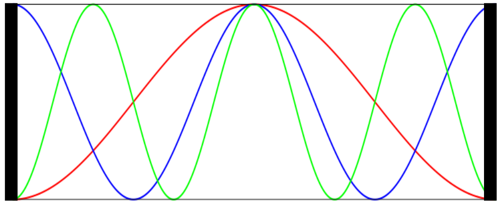

Circuit representation

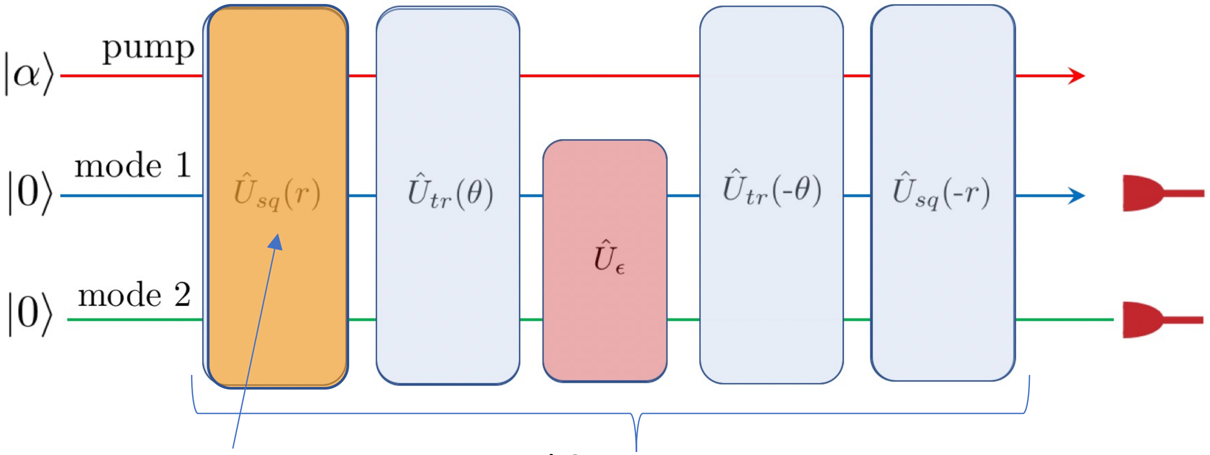

Sabin et al 2014 Howl & Fuentes AVS Quantum Science 2023

Improves the sensitivity by several orders of magnitude.
Squeezing can be much smaller than assumed previously and the system can suffer from short phononic lifetimes.

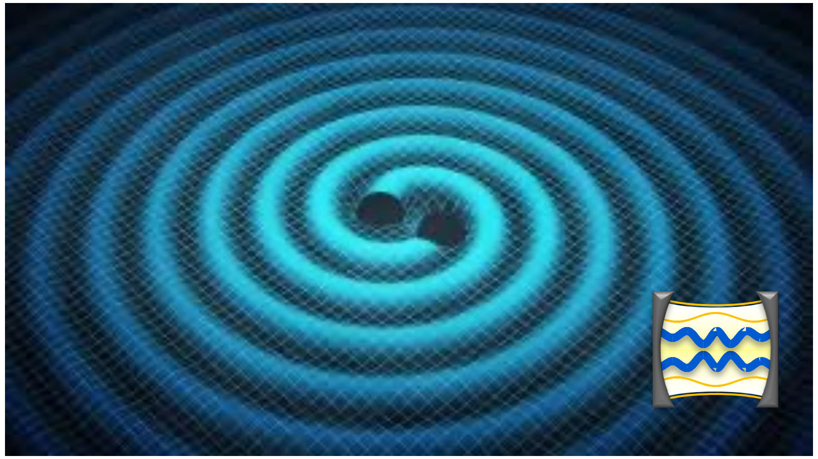

Interferometric transformations

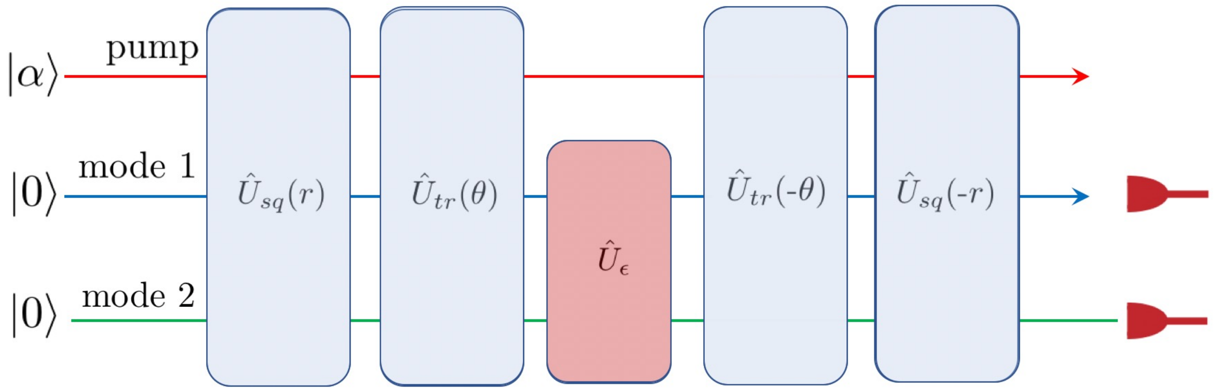

Two-mode squeezing operation

$$\boldsymbol{S}_s = \begin{pmatrix} \mathbf{1} & \mathbf{0} & \mathbf{0} \\ \mathbf{0} & \cosh r\mathbf{1} & \sinh r(\cos\vartheta_{sq}\boldsymbol{\sigma_z} + \sin\vartheta_{sq}\boldsymbol{\sigma_x}) \\ \mathbf{0} & \sinh r(\cos\vartheta_{sq}\boldsymbol{\sigma_z} + \sin\vartheta_{sq}\boldsymbol{\sigma_x}) & \cosh r\mathbf{1} \end{pmatrix},$$

The tritter transformation is

$$\boldsymbol{S}_{tr} = \begin{pmatrix} \cos\theta\mathbf{1} & \frac{1}{\sqrt{2}}\sin\theta(\sin\vartheta\mathbf{1} + i\cos\vartheta\boldsymbol{\sigma_y}) & \frac{1}{\sqrt{2}}\sin\theta(\sin\vartheta\mathbf{1} + i\cos\vartheta\boldsymbol{\sigma_y}) \\ -\frac{1}{\sqrt{2}}\sin\theta(\sin\vartheta\boldsymbol{\sigma_z} - i\cos\vartheta\boldsymbol{\sigma_y}) & \cos^2(\frac{\theta}{2})\mathbf{1} & -\sin^2(\frac{\theta}{2})\mathbf{1} \\ -\frac{1}{\sqrt{2}}\sin\theta(\sin\vartheta\boldsymbol{\sigma_z} - i\cos\vartheta\boldsymbol{\sigma_y}) & -\sin^2(\frac{\theta}{2})\mathbf{1} & \cos^2(\frac{\theta}{2})\mathbf{1} \end{pmatrix}.$$

Howl & Fuentes [arXiv:1902.09883](https://arxiv.org/abs/1902.09883)

Application: gravitational wave detector

Three mode application

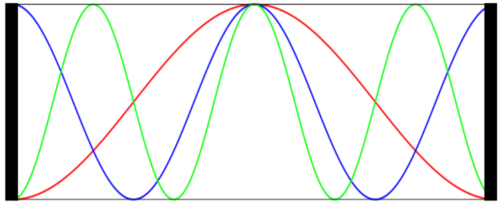

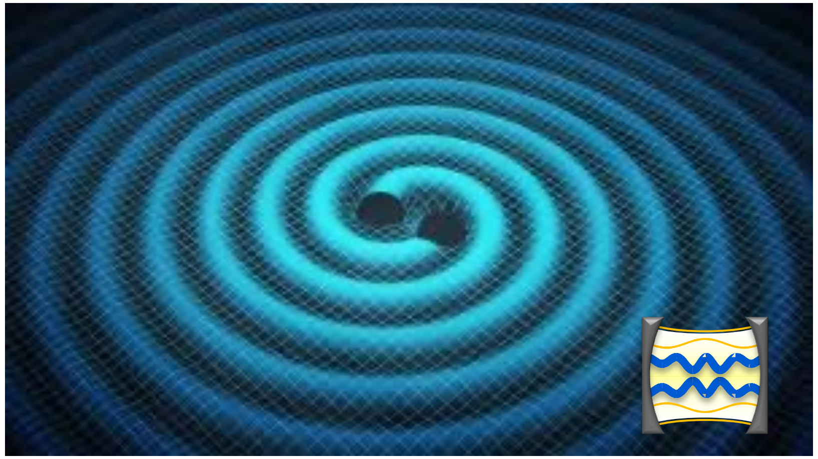

Interferometric transformations

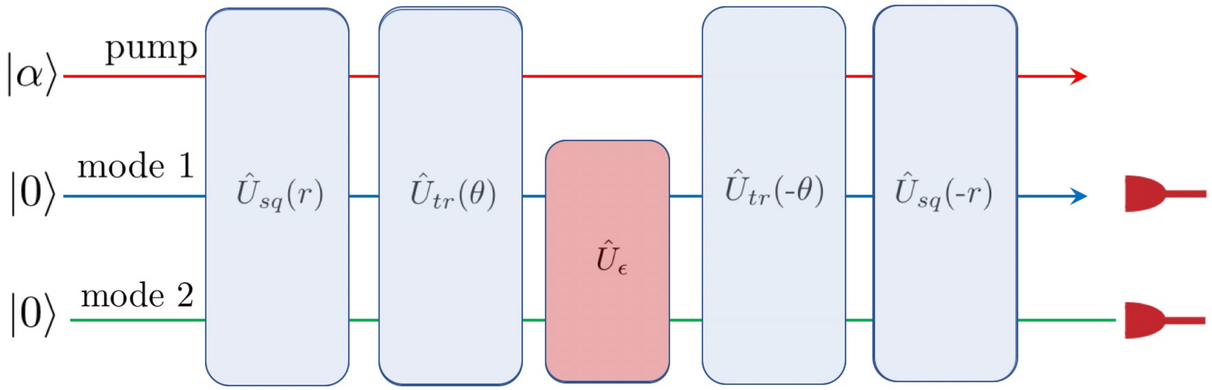

Two-mode squeezing operation

$$\boldsymbol{S}_s = \begin{pmatrix} \mathbf{1} & \mathbf{0} & \mathbf{0} \\ \mathbf{0} & \cosh r\mathbf{1} & \sinh r(\cos\vartheta_{sq}\boldsymbol{\sigma_z} + \sin\vartheta_{sq}\boldsymbol{\sigma_x}) \\ \mathbf{0} & \sinh r(\cos\vartheta_{sq}\boldsymbol{\sigma_z} + \sin\vartheta_{sq}\boldsymbol{\sigma_x}) & \cosh r\mathbf{1} \end{pmatrix},$$

The tritter transformation is

$$\boldsymbol{S}_{tr} = \begin{pmatrix} \cos\theta\mathbf{1} & \frac{1}{\sqrt{2}}\sin\theta(\sin\vartheta\mathbf{1} + i\cos\vartheta\boldsymbol{\sigma_y}) & \frac{1}{\sqrt{2}}\sin\theta(\sin\vartheta\mathbf{1} + i\cos\vartheta\boldsymbol{\sigma_y}) \\ -\frac{1}{\sqrt{2}}\sin\theta(\sin\vartheta\boldsymbol{\sigma_z} - i\cos\vartheta\boldsymbol{\sigma_y}) & \cos^2(\frac{\theta}{2})\mathbf{1} & -\sin^2(\frac{\theta}{2})\mathbf{1} \\ -\frac{1}{\sqrt{2}}\sin\theta(\sin\vartheta\boldsymbol{\sigma_z} - i\cos\vartheta\boldsymbol{\sigma_y}) & -\sin^2(\frac{\theta}{2})\mathbf{1} & \cos^2(\frac{\theta}{2})\mathbf{1} \end{pmatrix}.$$

Howl & Fuentes Howl & Fuentes AVS Quantum Science 2023

Quantum metrology

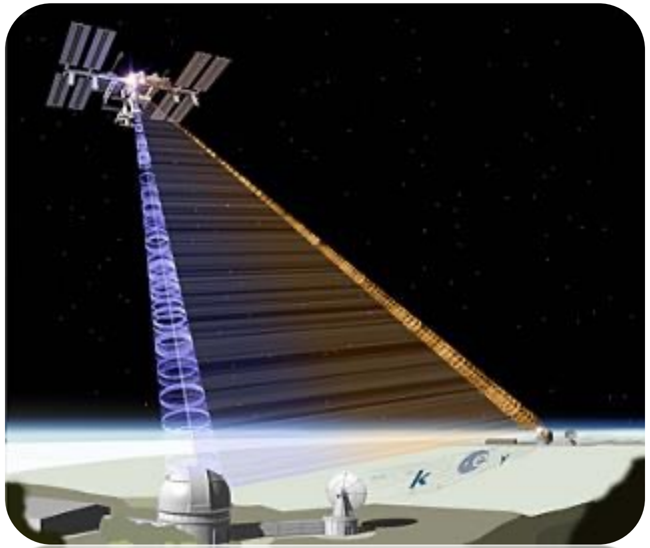

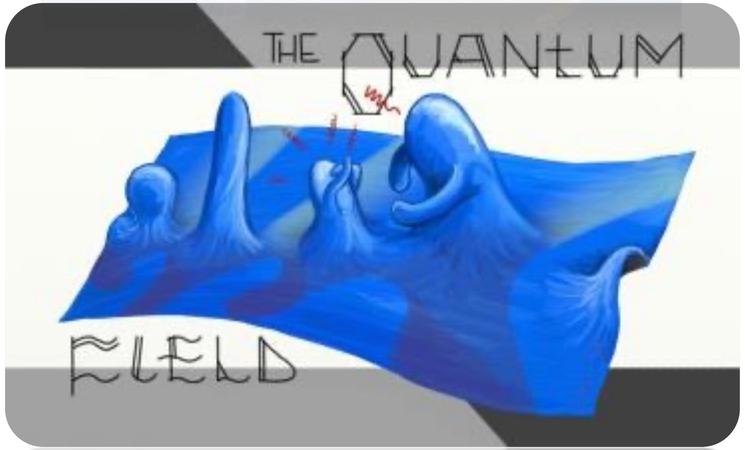

- Enables ultrasensitive devices for measuring fields, frequencies, time
- Quantum clocks and sensors are being sent to space… relativity cannot be ignored

Used to measure gravitational parameters…

gravitational field strengths
accelerations

Quantum Metrology

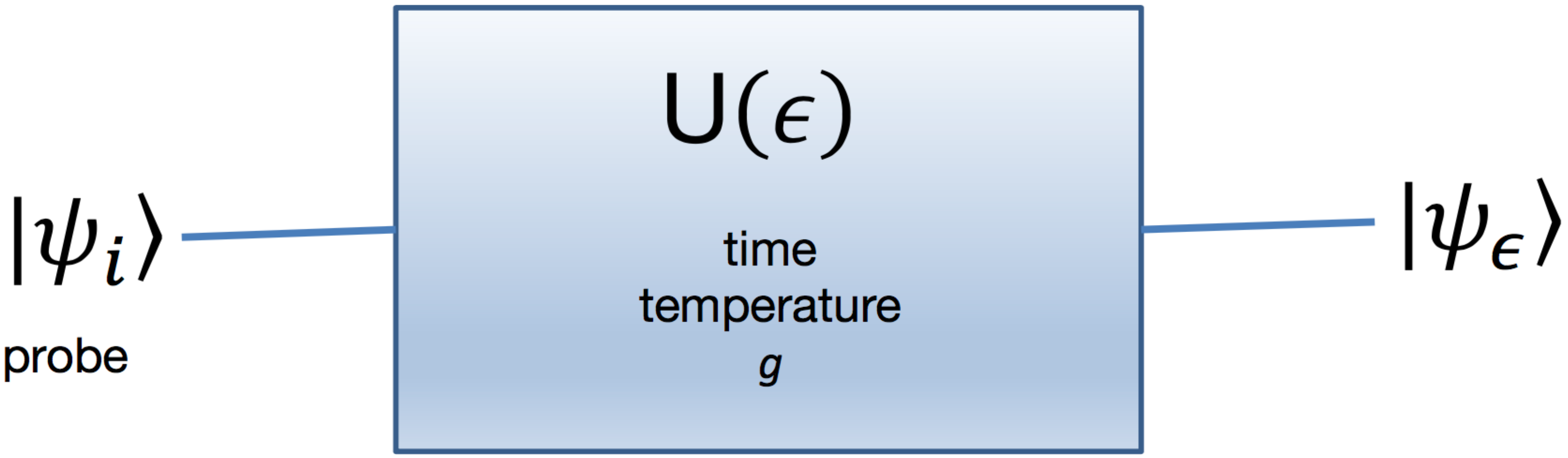

$$\langle \psi_\epsilon | \psi_{\epsilon + d\epsilon} \rangle \ll 1$$

Exploit quantum properties of the probe state to estimate with high precision parameters in the theory (Hamiltonian)

Quantum Metrology

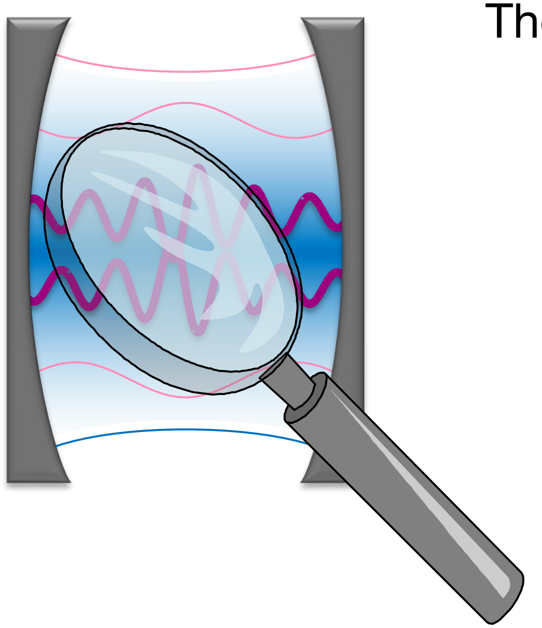

There is an optimal measurement such that

parameter

$$\langle (\Delta\hat{\epsilon})^2 \rangle \geq \frac{1}{M H_\epsilon}$$

Error

Quantum Fisher information

M number of measurements

$$H_\epsilon = \frac{8\left(1 - \sqrt{\mathcal{F}(\sigma_\epsilon, \sigma_{\epsilon+d\epsilon})}\right)}{d\epsilon^2}$$

Fidelity

state σ_ϵ

$\langle \psi_\epsilon | \psi_{\epsilon+d\epsilon} \rangle \ll 1$

General framework for RQM

Ahmadi, Bruschi, Sabin, Adesso, Fuentes, Nature Sci. Rep. 2014
Ahmadi, Bruschi, Fuentes PRD 2014

Fisher information in QFT:
Analytical formulas in terms of
general Bogoliubov coefficients

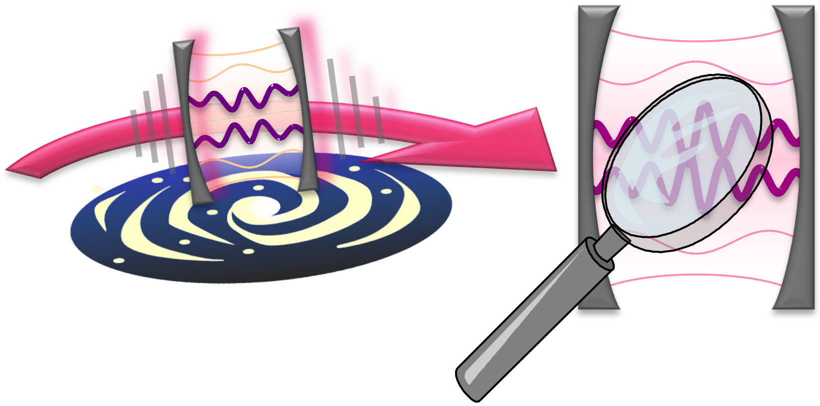

Single-mode
Two-mode channels

for small parameters

$$
\begin{aligned}
H &= \epsilon^{-2}\Re\Big[4\cosh r(f_\alpha^n + f_\beta^n + f_\alpha^m + f_\beta^m) \\
&+ 4\cosh^2 r(2|\beta_{nm}(t)|^2 - f_\alpha^n + f_\beta^n - f_\alpha^m + f_\beta^m) \\
&- 4\sinh^2 r(-f_\alpha^n + f_\beta^n - f_\alpha^m + f_\beta^m + 2\beta_{nm}(t)^2 - 2\alpha_{nm}(t)^2) \\
&+ 4\sinh r\,\Re[\mathcal{G}_{nm}^{\alpha\beta} + \mathcal{G}_{nm}^{\alpha\beta}] - 4\cosh^4 r|\beta_{nm}(t)|^2 \\
&- \frac{1}{2}\sinh^2 2r(2|\alpha_{nm}(t)|^2 - 3|\beta_{nm}(t)|^2 - \beta_{nm}(t)^2\Big].
\end{aligned}
$$

$$
\begin{aligned}
f_\alpha^i &= \frac{1}{2}\sum_{n\neq k,k'} |\alpha_{ni}|^2 \\
f_\beta^i &= \frac{1}{2}\sum_{n\neq k,k'} |\beta_{ni}|^2 \\
\mathcal{G}_{ij}^{\alpha\beta} &= \sum_{n\neq k,k'} \alpha_{ni}\beta_{nj}^*
\end{aligned}
$$

Detector sensitivity

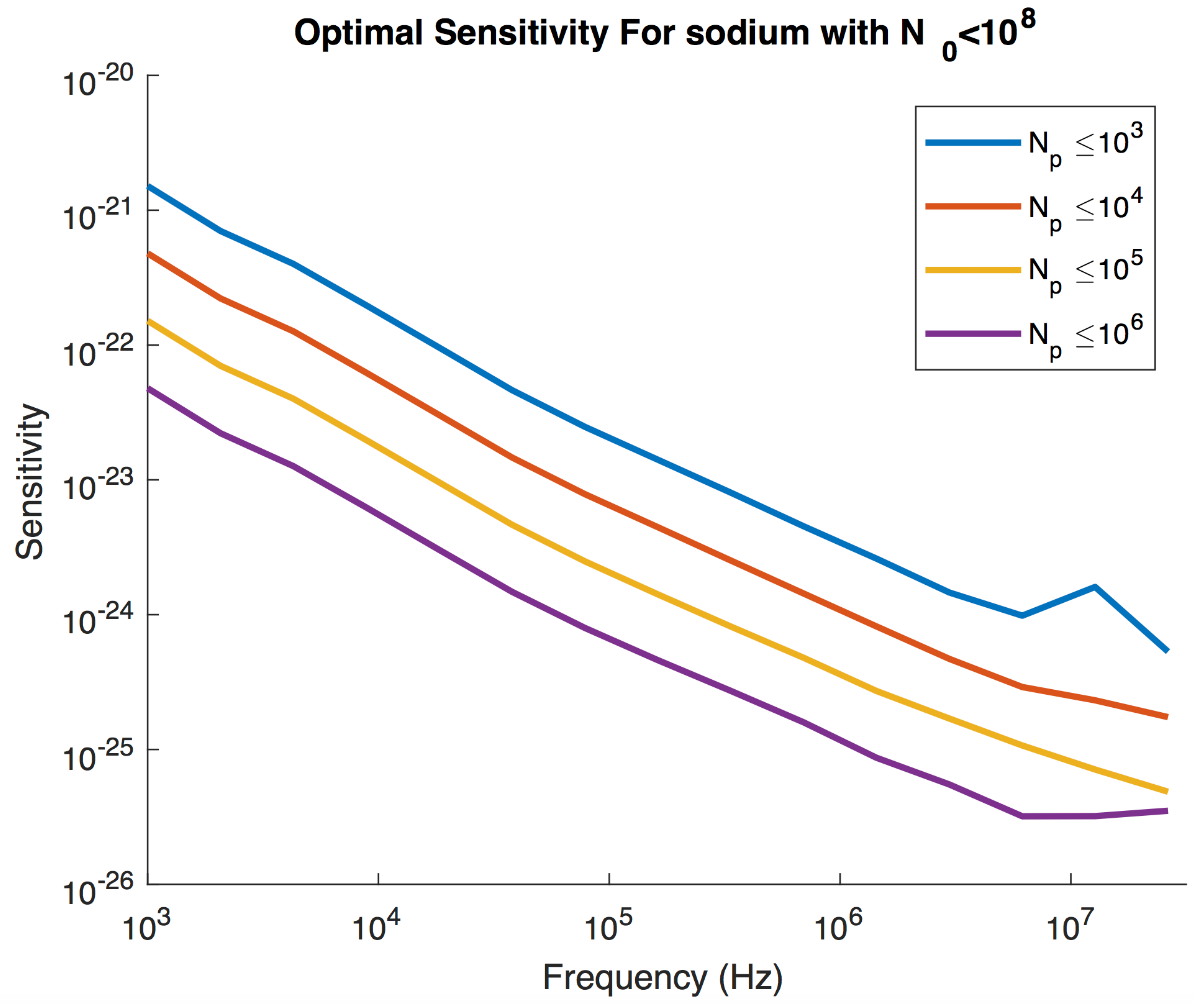

$$\Delta\epsilon \geq \frac{1}{\sqrt{MF_Q}}$$

$$\Delta\epsilon \geq \frac{m}{\sqrt{2\pi\hbar}}\frac{\alpha^3}{\theta N_0^2\sqrt{N_p\tau t}}\sqrt{\frac{L^7}{a^3}}\frac{\sqrt{nl}\,(l-n)^2}{(l^2+n^2)}$$

m atomic mass
θ tritter angle
N_0 number of atoms in the ground state
N_p number of phonons in the two-mode squeezed state
$\alpha = \sqrt{A}/L$, A area, L length
a scattering length
$M = \tau/t$ number of measurements
τ integration time
t interaction time (lifetime of the phonons)
$\Omega = \omega_n + \omega_l$ the frequency of the gw
$\omega_j = j\pi c_s/L$ phonon frequency
n, l mode numbers

Howl & Fuentes arXiv:1902.09883

Detector sensitivity

Figure 8. Spectrum of gravitational wave sources [18, 22]. In this figure, the abbreviations are: BH, collapse to black hole; NS/NS, neutron star coalescence; NS evol, secular evolution of a nonaxisymmetric neutron star.

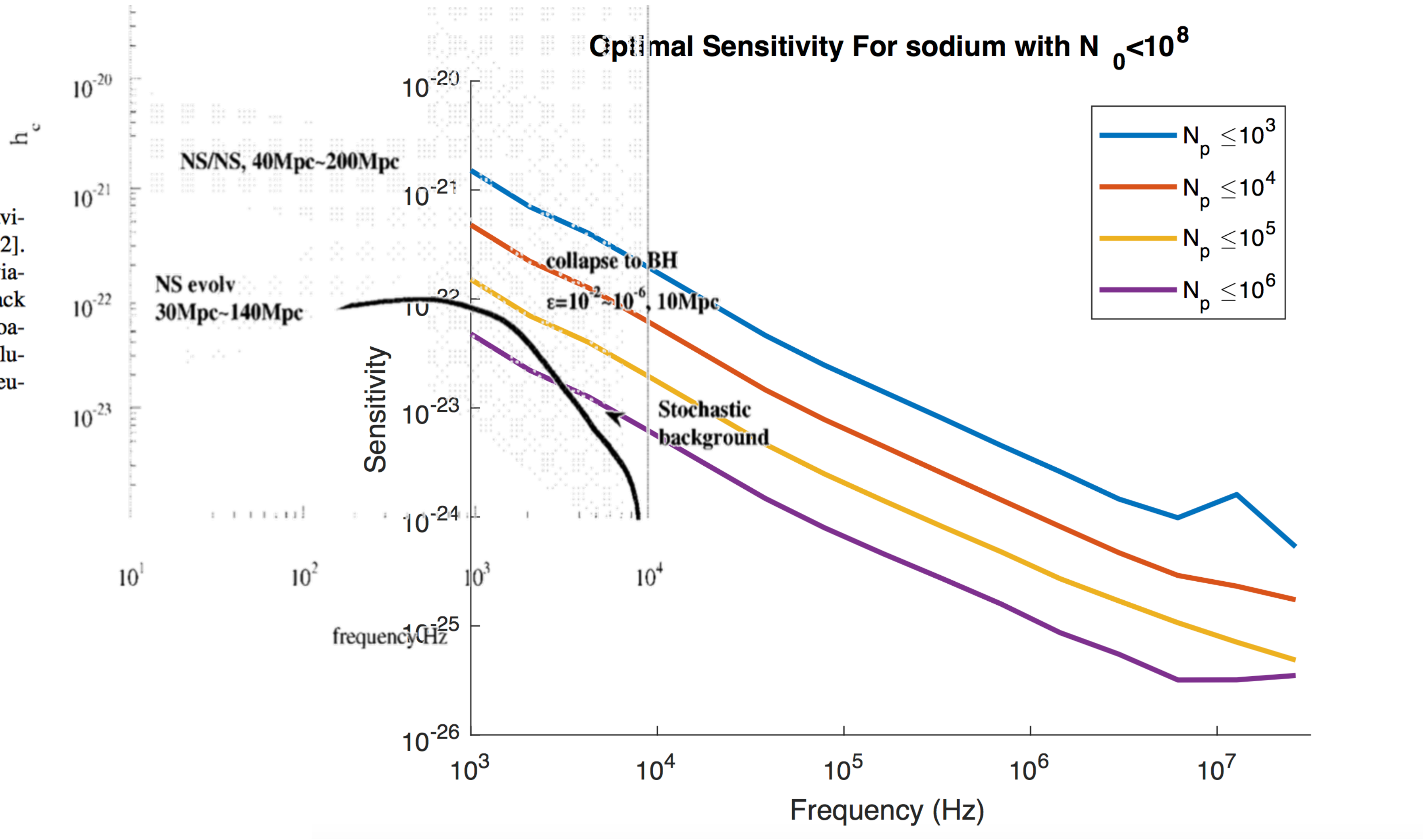

Constraints

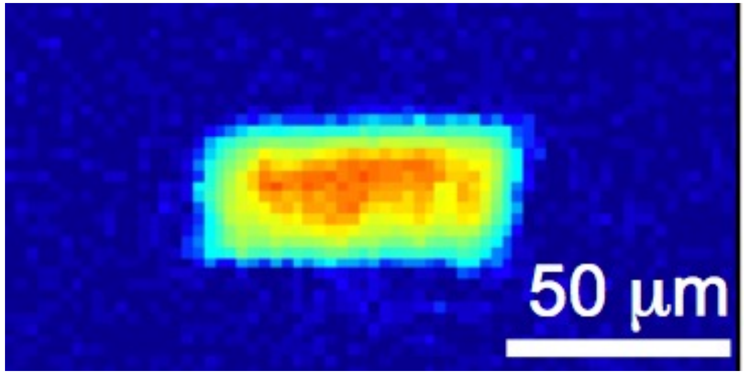

	$(\gamma^{La}_{k_BT\ll\mu})^{-1}$ (1.56)	$(\gamma^{La}_{k_BT\gg\mu})^{-1}$ (1.56)	$(\gamma^{Be,0})^{-1}$ (1.55)	$t_{1/2}$ (3.3)
$t \approx$	$\frac{640}{3\pi}\frac{\hbar^7\beta^4 L n_0^3 a_s^2}{l m^3}$	$\frac{8}{\pi}\frac{\beta L}{a_s l}$	$\frac{640}{3\pi^6}\frac{m L^5 n_0}{\hbar l^5}$	$\frac{1}{50}\frac{m}{\hbar n_0^2 a_s^4}$
$r \propto$	$\frac{\hbar^8\beta^4 L^2 n_0^{9/2} a_s^{7/2}}{l^2 m^4}$	$\frac{\hbar^2 L^2 \beta n_0^{3/2} a_s^{1/2}}{l^2 m}$	$\frac{L^6 n_0^{5/2} a_s^{3/2}}{l^6}$	$\frac{L}{l n_0^{1/2} a_s^{5/2}}$
$\beta\omega_l$	$2\sqrt{\pi}\frac{\hbar l\sqrt{n_0 a_s}}{Lm}$		weak interactions	$\lvert a_s\rvert n_0^{1/3} \ll 1$
phonon regime	$\sqrt{\frac{\pi l^2}{L^2 n_0 a_s}} \ll 1$		ultracold regime	$\frac{1}{4\pi}\frac{m}{\hbar^2\beta\, n_0\, a_s} \ll 1$

Table 8.2: Approximate values for the limitations to the phonon and condensate life times and resulting proportionalities of the maximum two-mode squeeze factor from SECTION 8.1 in the case where the respective damping or particle losses become dominant.
The two bottom rows show a measure $\beta\omega_l$ for the thermal occupation of the initial state, which should be minimal, and restrictions from the diluteness condition and the assumptions of the phononic and the ultracold regime.
To see where one could optimize and which boundaries will be encountered, all quantities above are given in terms of the parameters characterizing an individual experiment.

Quantum decoherence of phonons in Bose–Einstein condensates

Richard Howl[1], Carlos Sabín[2], Lucia Hackermüller[3] and Ivette Fuentes[1,4]

Published 29 November 2017 • © 2017 IOP Publishing Ltd
Journal of Physics B: Atomic, Molecular and Optical Physics, Volume 51, Number 1
Citation Richard Howl *et al* 2018 *J. Phys. B: At. Mol. Opt. Phys.* **51** 015303

P. Juschitz, Two-mode Phonon Squeezing in Bose-Einstein Condensates for Gravitational Wave Detection arXiv:2101.05051

Search for yet unknow sources

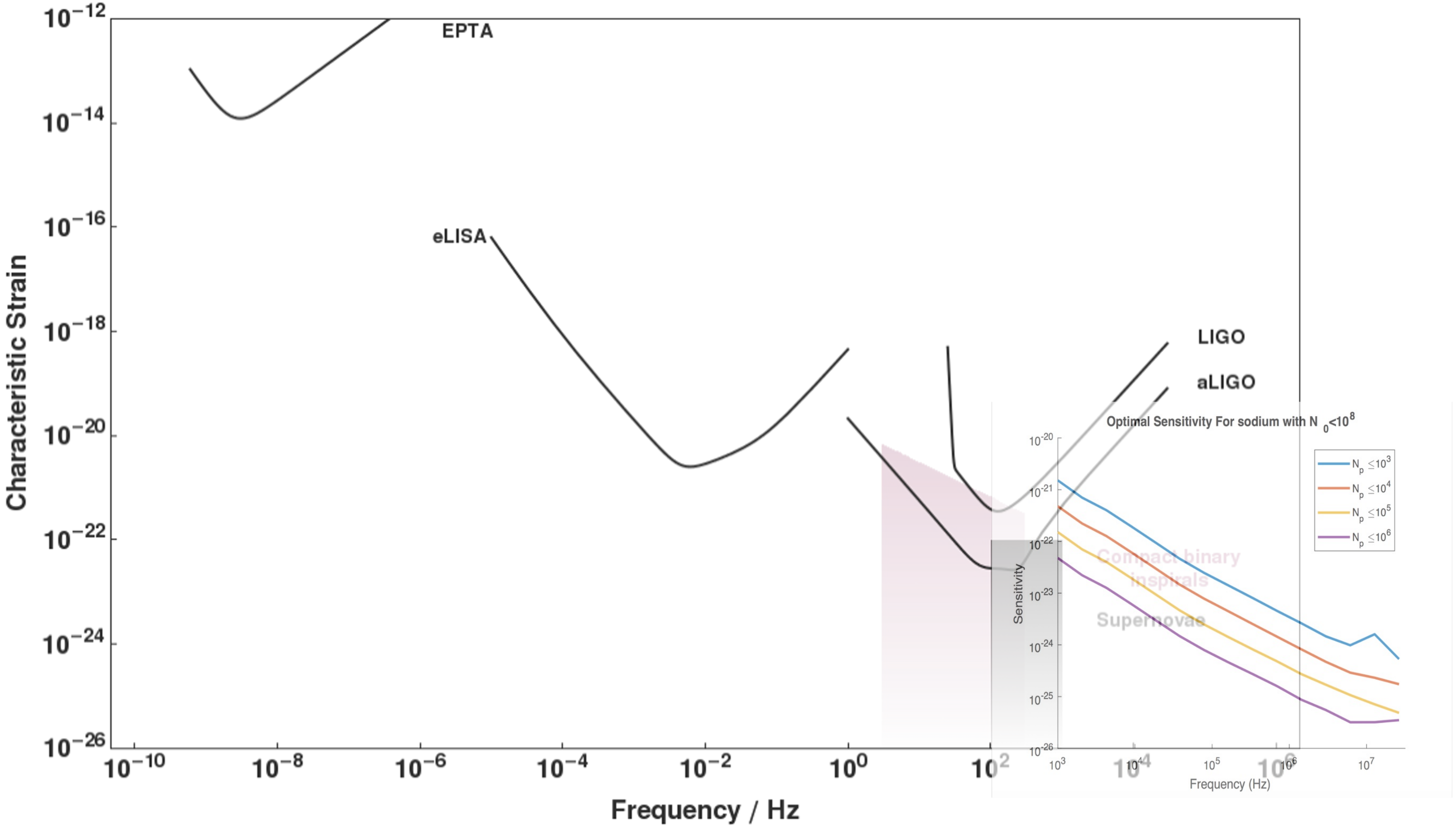

Know sources: 10 kHz

Exotic sources:
primordial black holes
boson stars
Early Universe Cosmology
Phase transitions
Preheating after inflation,
Cosmic strings
Dark matter
Ultralight 10^{-8}- 10^{14} Hz
Decay: Penrose CCC

Ultra-Light Dark Matter
(bosonic)

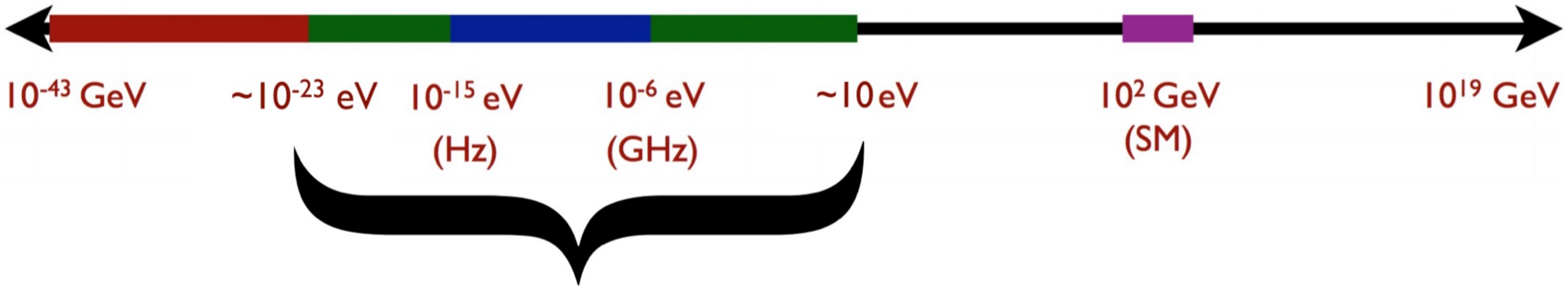

→ search for *coherent effects of the entire field*, not single hard particle scatterings

Generic Candidates: Light pseudo-Nambu-Goldstones (axions and "axion like particles" — ALPs); Massive hidden vector bosons (aka "dark photons"); Light scalars (moduli/dilatons…)

Slide by John March-Russel

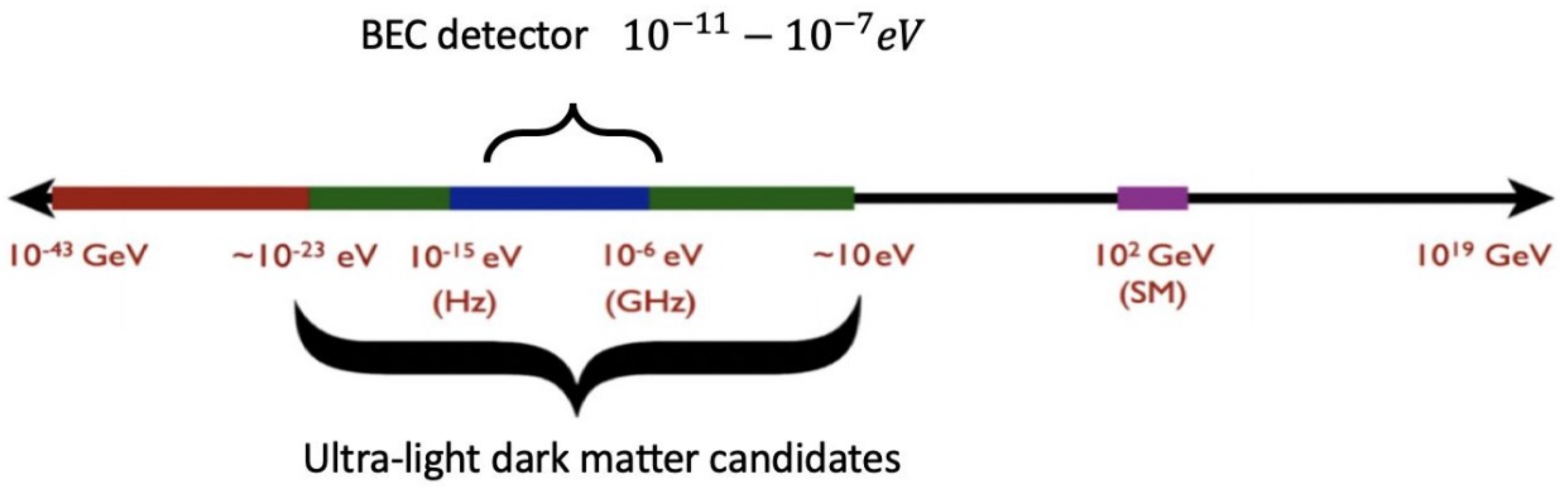

BEC detector $10^{-11} - 10^{-7} eV$
10^{-43} GeV
$\sim 10^{-23}$ eV
10^{-15} eV
(Hz)
10^{-6} eV
(GHz)
~ 10 eV
10^{2} GeV
(SM)
10^{19} GeV
Ultra-light dark matter candidates

Different principle

Interferometer arm length L

$$\frac{\Delta L}{L}$$

Resonance

$$\Omega = \omega_n + \omega_m$$

wave

quantum excitations

Quantum Weber Bar

Temperature

Weber bar

$T \sim 4\ K$

BEC

$T \sim 5x10^{-10} K$

Initial quantum states
Squeezing
Parametric amplification

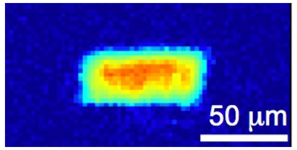

How can it work if its so small?

$$\omega \sim \frac{C_s}{L}$$

$$\omega \sim \frac{C}{L}$$

Speed of sound: $C_s = 10\mathrm{mm/s}$
$L = 10^{-1}$-$10^{-3}\mathrm{mm}$

Speed of light: C= $2.99\mathrm{x}10^{11}$mm/s
L =2.99Km-2990Km

Broadband: 3D

Spherical BEC

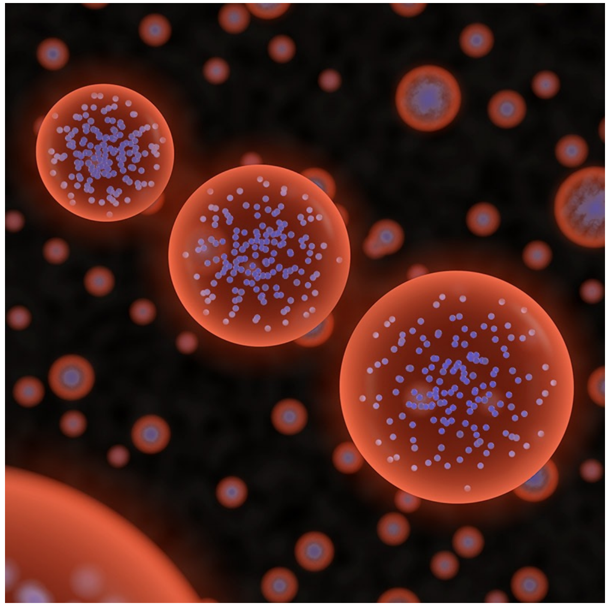

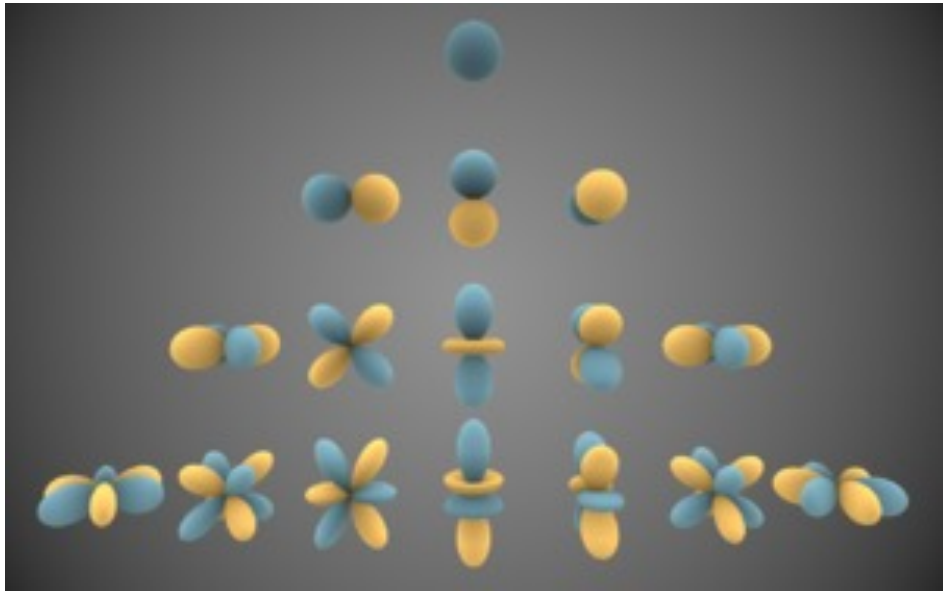

We are studying different geometries

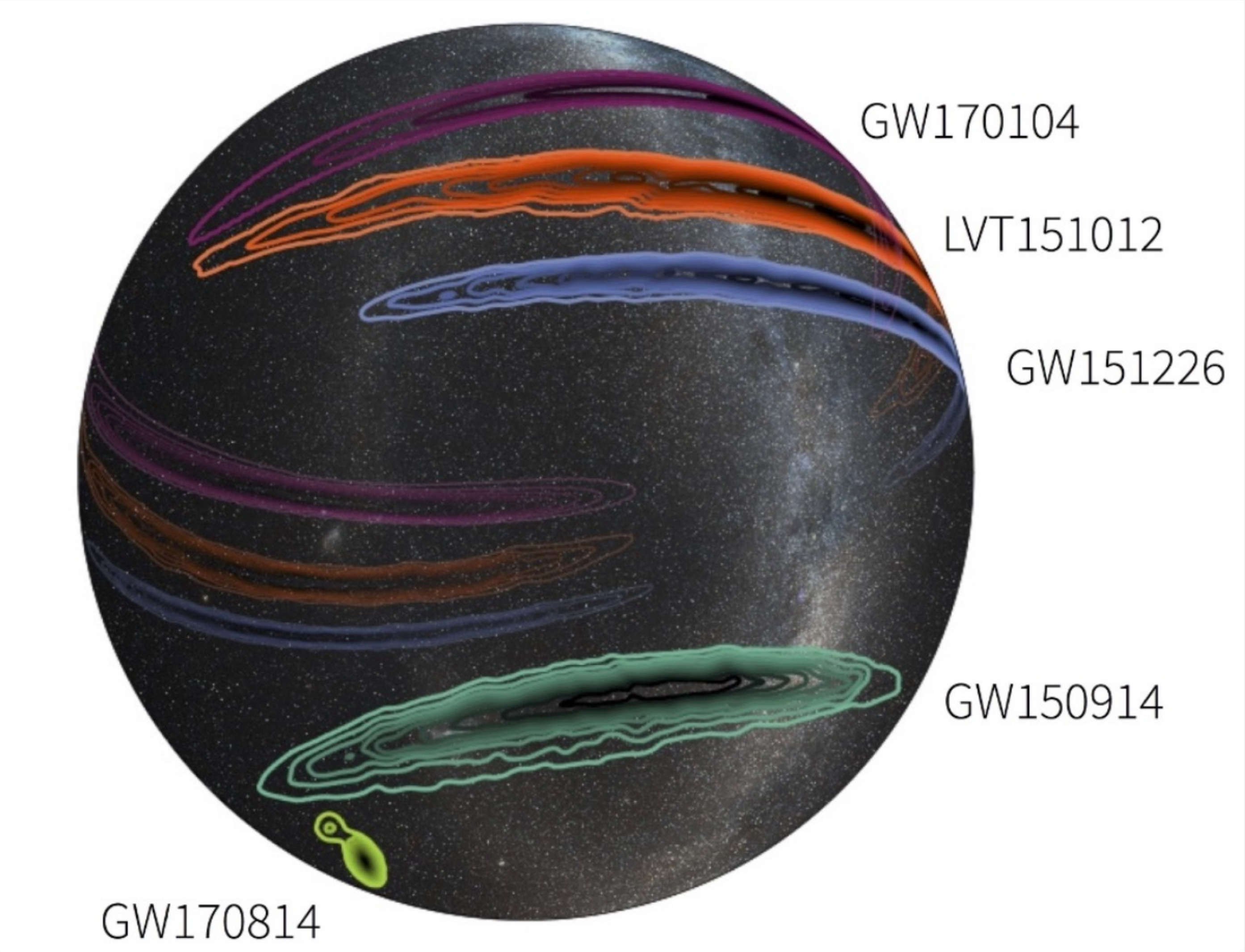

This three-dimensional projection of the Milky Way galaxy onto a transparent globe shows the probable locations of the three confirmed black-hole merger events observed by the two LIGO detectors—GW150914 (dark green), GW151226 (blue), GW170104 (magenta)—and a fourth confirmed detection (GW170814, light green, lower-left) that was observed by Virgo and the LIGO detectors. Also shown (in orange) is the lower significance event, LVT151012. Image credit: LIGO/Virgo/Caltech/MIT/Leo Singer (Milky Way image: Axel Mellinger).

Commercial applications

$$g = \mathrm{diag}\left(-f(r), \frac{1}{f(r)}, r^2, r^2 \sin^2\vartheta\right)$$

$$f(r) = 1 - r_S/r$$

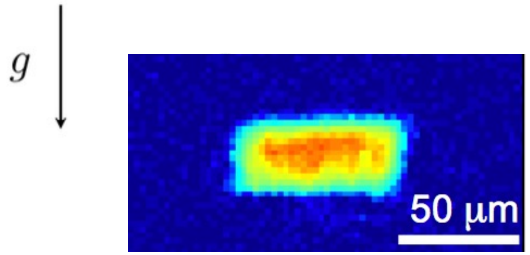

Phononic gravimeter:
Same sensitivity but much smaller system.

Phononic gradiometer:
Improves the state of the art by at least two orders of magnitude

1. WO2020249974 - QUANTUM GRAVIMETERS AND GRADIOMETERS

PCT Biblio. Data | Description | Claims | Drawings | ISR/WOSA/A17(2)(a) | National Phase | Notices | Documents

Submit observation PermaLink

Report Type: International Search Report in XML ▼ Report Language: English - Original Document ▼

Disclaimer The image version (PDF) available on PATENTSCOPE is the official version. This online html version is provided to assist users. Despite the great care taken in its compilation to ensure a precise and accurate representation of the data appearing on the printed document/images, errors and/or omissions cannot be excluded due to the data transmittal, conversion and inherent limitations of the (optional) machine translation processes used. Hyperlinks followed by this symbol, are to external resources that are not controlled by WIPO. WIPO disclaims all liability regarding the above points.

Part 1: 1 2 3 4 5 6 Part 2: A B C D E

PATENT COOPERATION TREATY
PCT
INTERNATIONAL SEARCH REPORT
(PCT Article 18 and Rules 43 and 44)

International application No.	Applicant's or agent's file reference
PCT/GB2020/051434	DJC96140P.WO
International filing date (day/month/year) 12 June 2020	(Earliest) Priority Date (day/month/year) 13 June 2019

Setup	Running time	Length	$\Delta r_S/r_S$
[14, 15, 17] Atom. Int.	100 s – 8 h	0.2 – 2.5 m	10^{-9}
[16] BEC-chip	100 s	10^{-2} m	10^{-10}
Phononic MZI	6 s	10^{-4} m	10^{-8}

Quantum technologies could be useful for Fundamental Physics

Main aim: Develop new instruments
window to scales that have not been explored before
New Physics!

Quantum technologies can help us put the pieces of the puzzle together

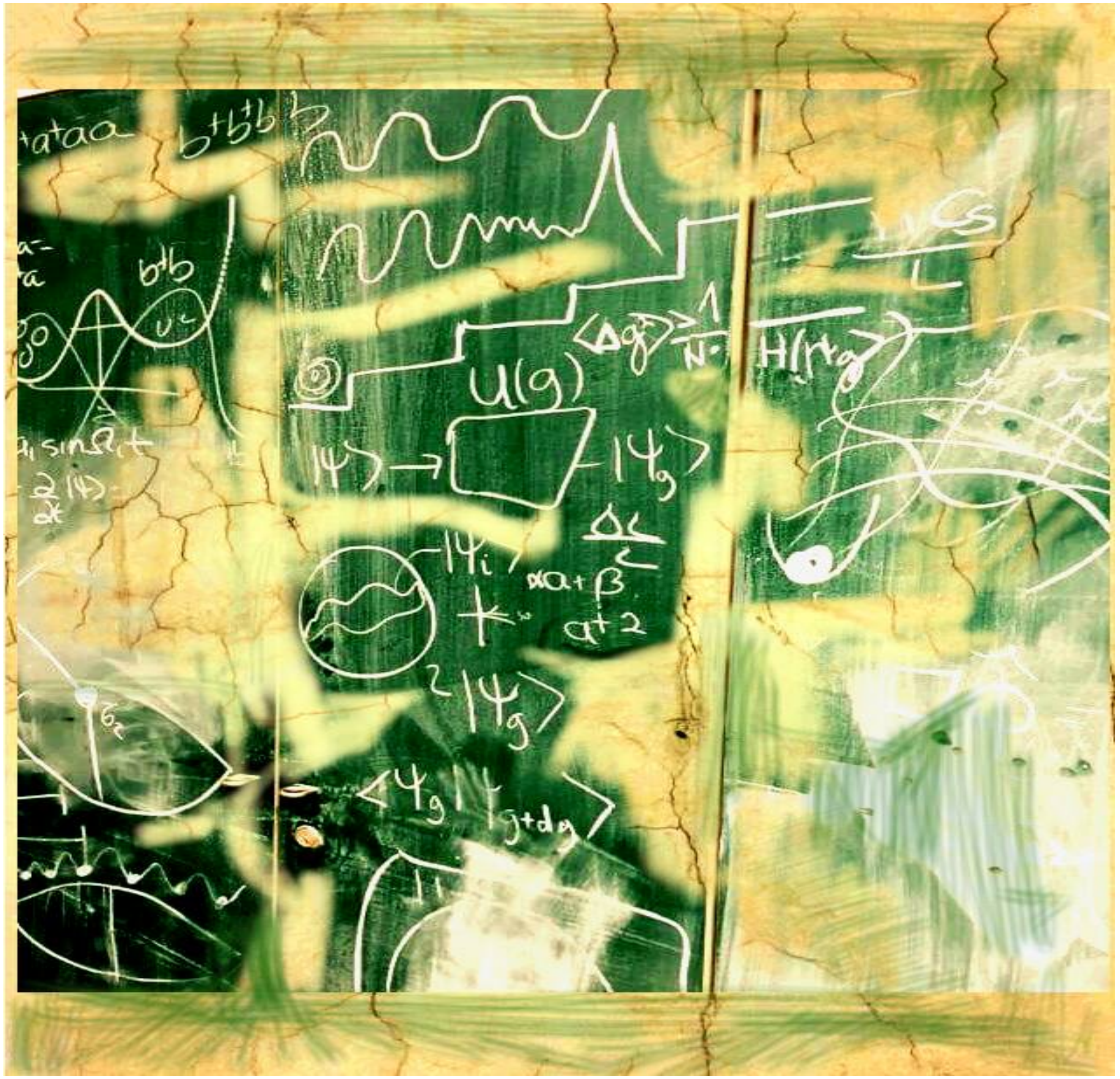

Relativistic effects
on
quantum clocks

Quantum clocks (quantum 1.0)

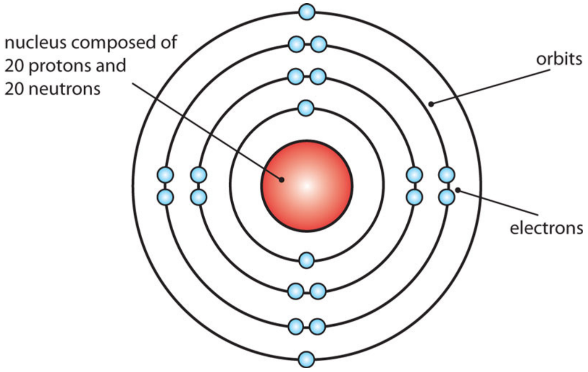

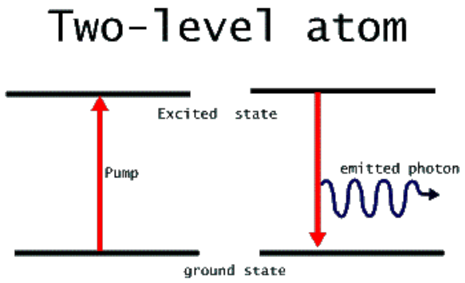

Optical clocks routinely achieving 10^{-17} - 10^{-18} systematic uncertainty

Time

Quantum mechanics

Time is absolute (Galilean trans.).

Space and time are different.

- Time is a parameter.
- Space is an operator.

Particles can be in a superposition of positions at once.

Relativity

Space and time are not different.

Time is observer dependent

Time flows at different rates in different points in space (Lorentz trans.)

Proper time

$$\Delta\tau = \int_P d\tau = \int_P \frac{1}{c}\sqrt{g_{\mu\nu}\, dx^\mu\, dx^\nu}$$

metric

Does quantum theory imposes fundamental limitations on how well we can measure proper time?

Einstein's light clock

Classical light

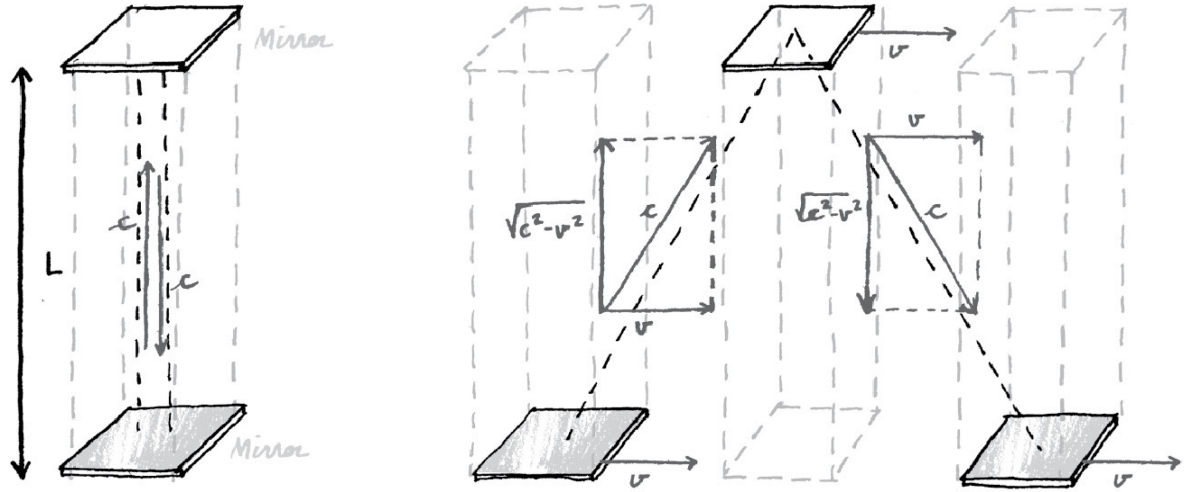

Quantum: photons

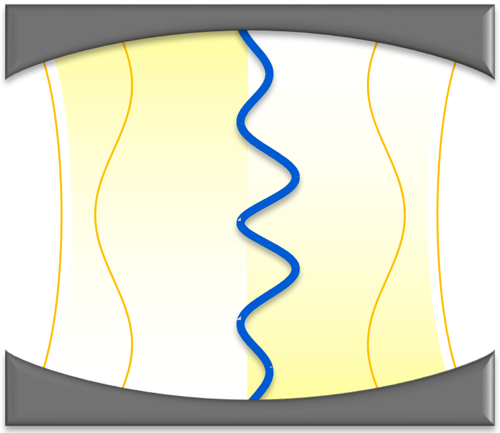

Lindkvist, Sabin, Fuentes, Dragan, Svensson, Delsing, Johansson PRA (2014)

Relativistic quantum clock model

Open Access | Published: 19 May 2015

Motion and gravity effects in the precision of quantum clocks

Joel Lindkvist, Carlos Sabín, Göran Johansson & Ivette Fuentes

Scientific Reports **5**, Article number: 10070 (2015) | Cite this article

Clock: one mode of the field
in a coherent or squeezed state

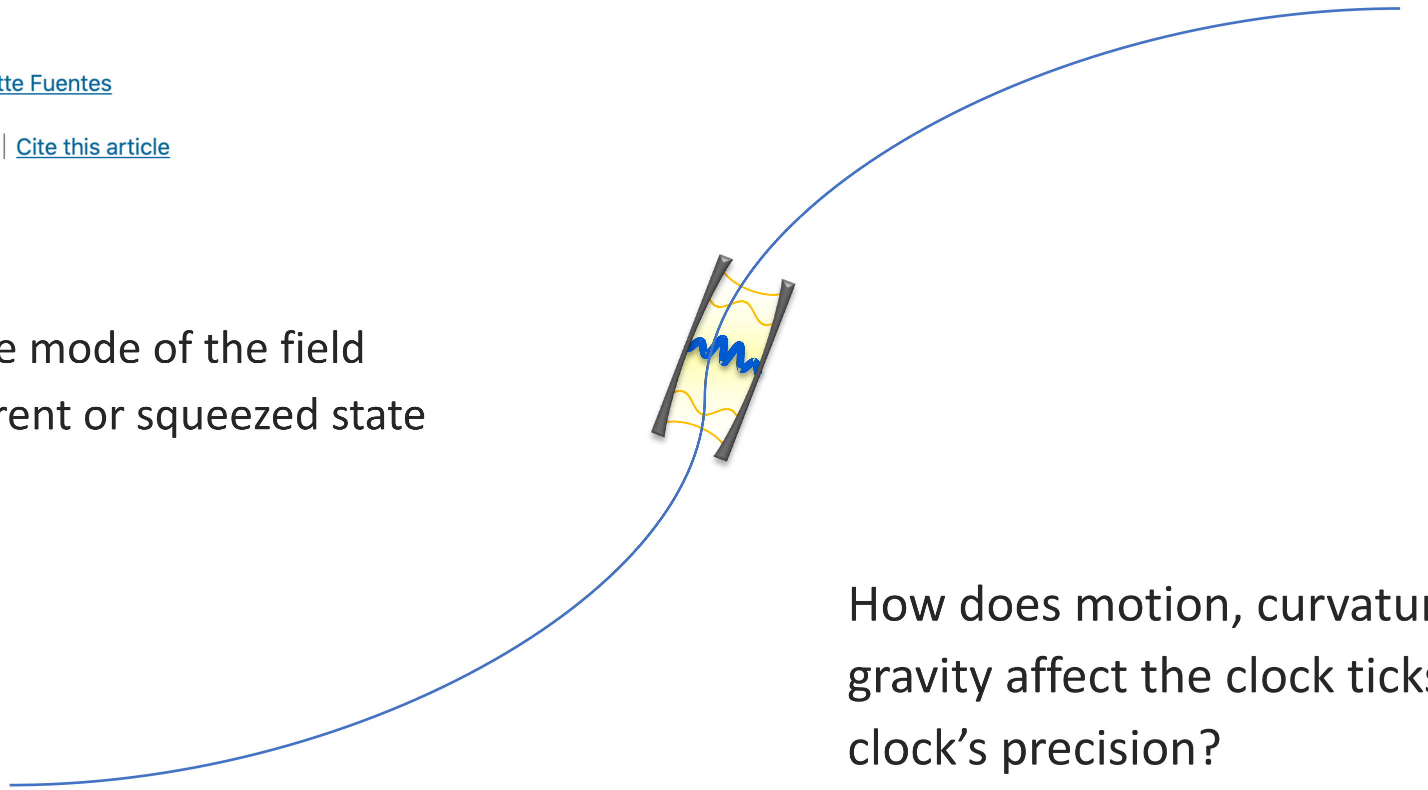

How does motion, curvature and gravity affect the clock ticks and the clock's precision?

Relativistic quantum clock model

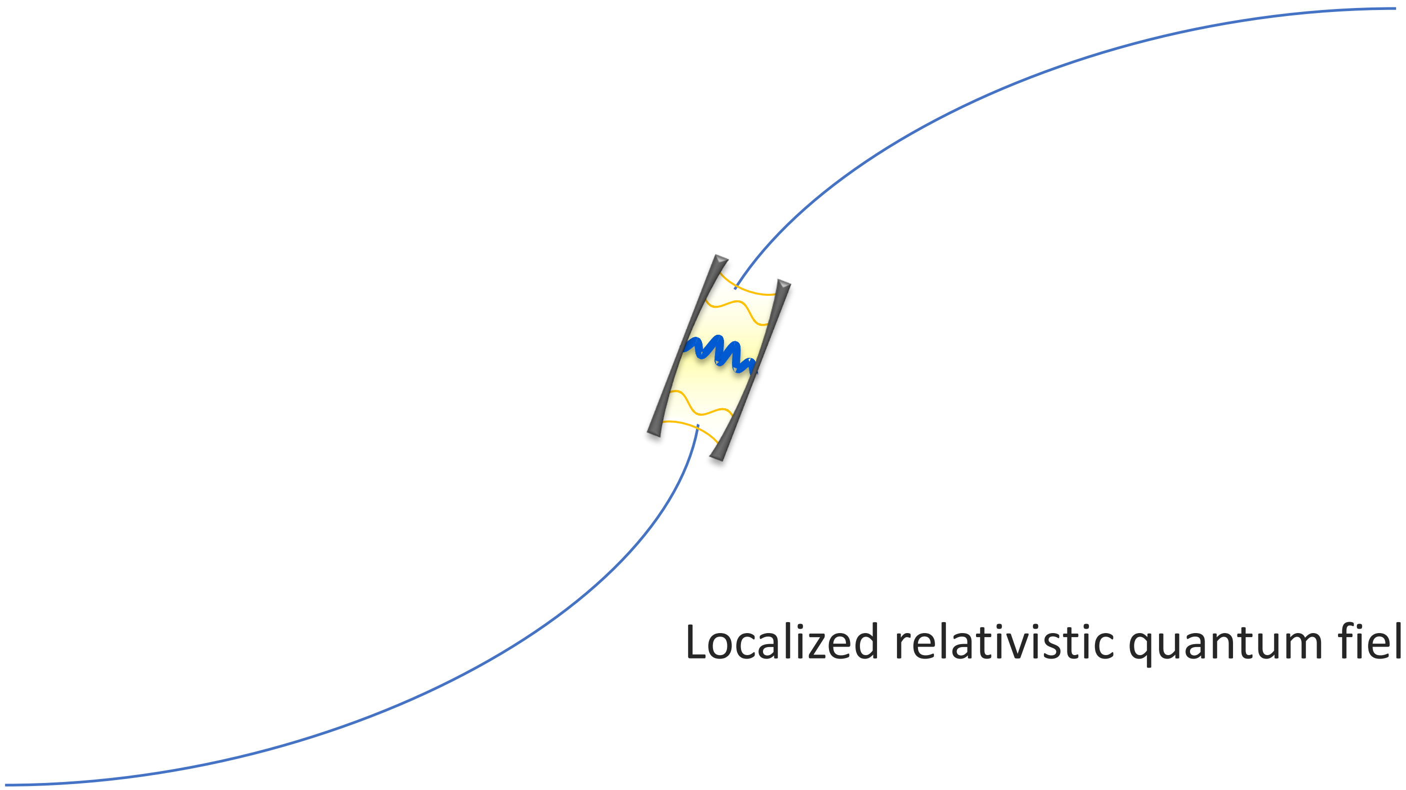

Localized relativistic quantum field

Relativistic quantum clock model

Clock: one mode of the field in a coherent state.

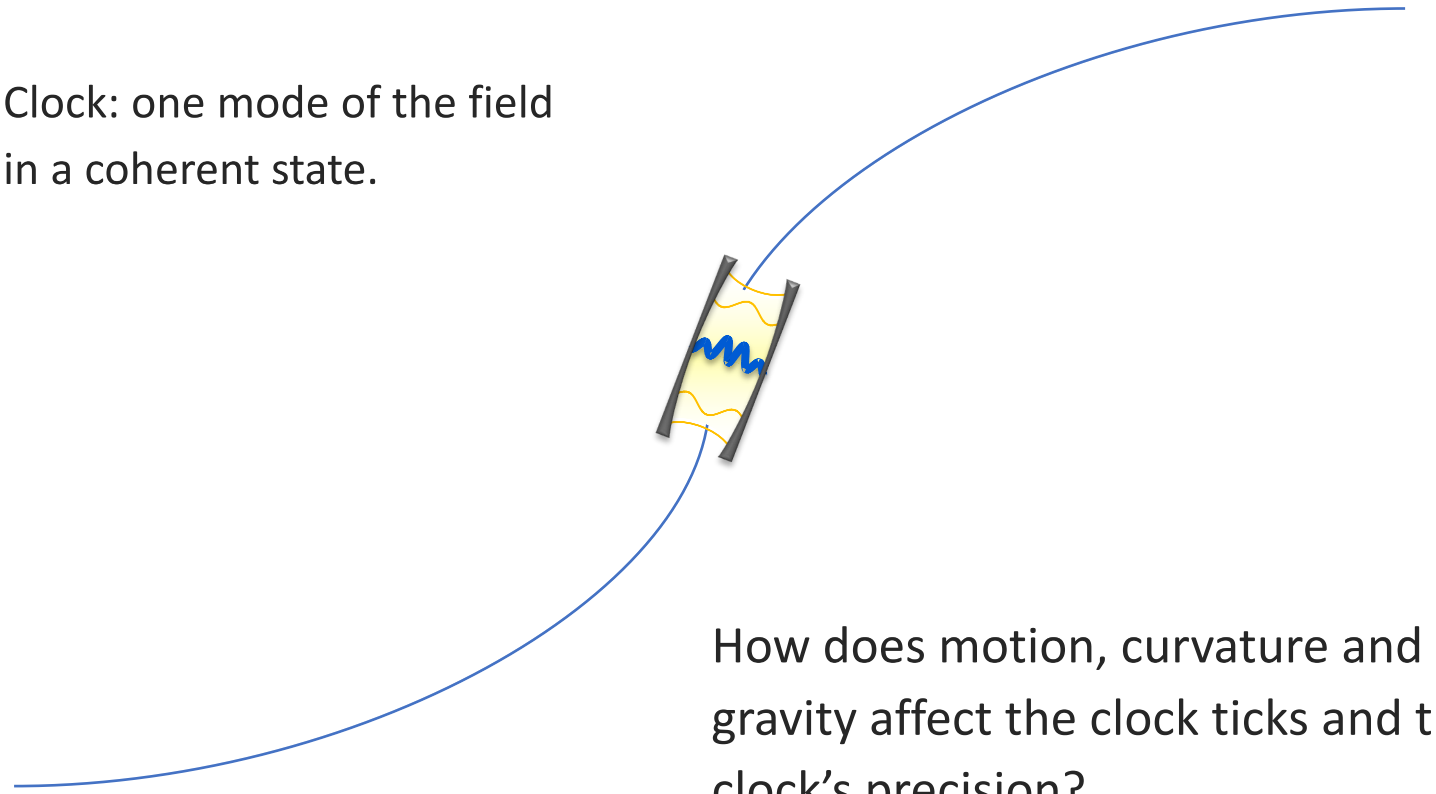

How does motion, curvature and gravity affect the clock ticks and the clock's precision?

Precision: Quantum Fisher information

Lindkvist, Sabin, Johansson and Fuentes, Sci. Rep. (2015)

$$H_\theta = 4\alpha^2 P\left[\cosh(2r) + \sinh(2r)\cos\phi\right] + \frac{4\sinh^2(2r)}{1+P^2} \qquad P = \frac{1}{4\sqrt{\det\sigma}}$$

Squeezing

Coherent state amplitude

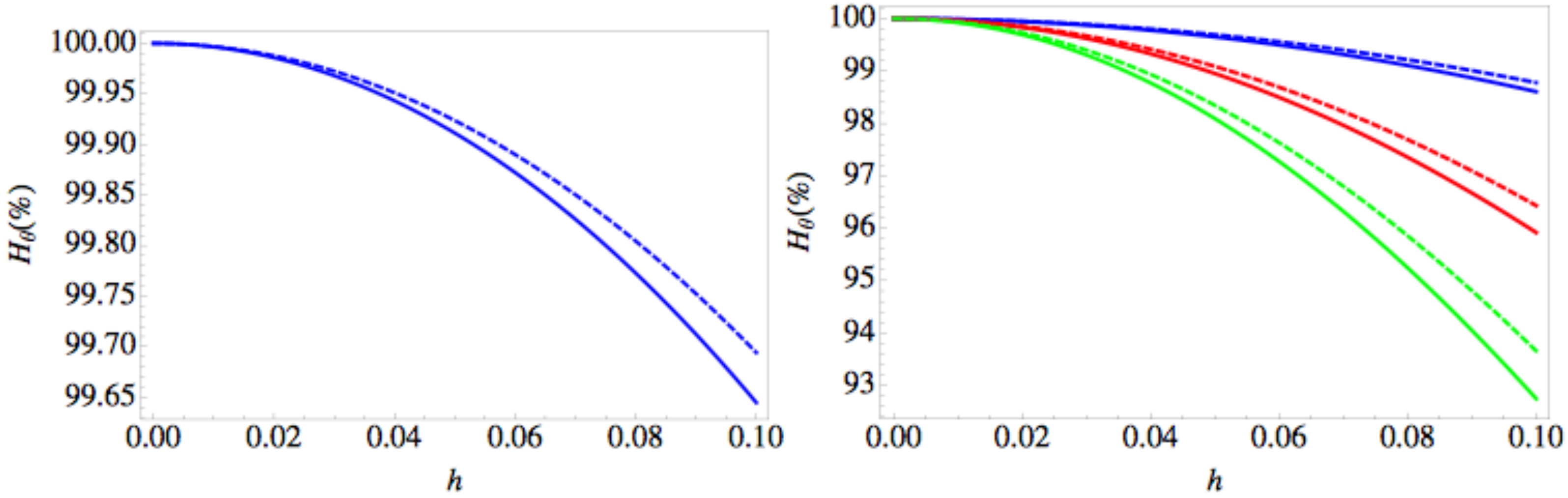

FIG. 2: a) Ratio of the transformed and original QFI for an initial coherent state as a function of h, for $\theta_a = \pi$ and initial photon numbers $N > 1$. The solid(dashed) curve is for $\theta_0 = 0(\pi/2)$. b) Ratio of the transformed and original QFI for an initially squeezed vacuum as a function of h, for $\theta_a = \pi$ and initial photon numbers $N = 1$ (blue), $N = 5$ (red) and $N = 10$ (green). The solid(dashed) curves are for $\theta_0 = 0(\pi/2)$.

Implementing the twin-paradox

Lindkvist, Sabin, Fuentes, Dragan, Svensson, Delsing, Johansson PRA (2014)

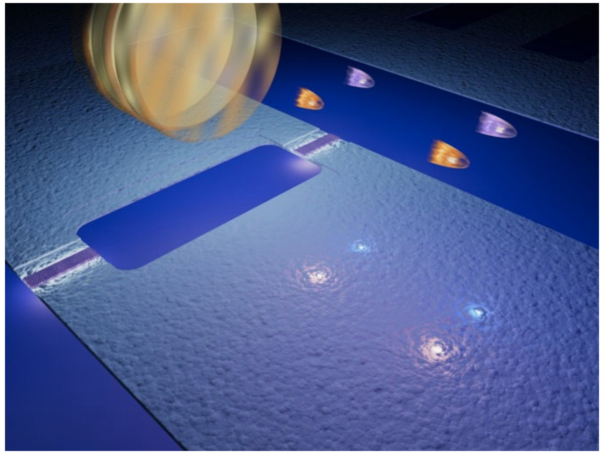

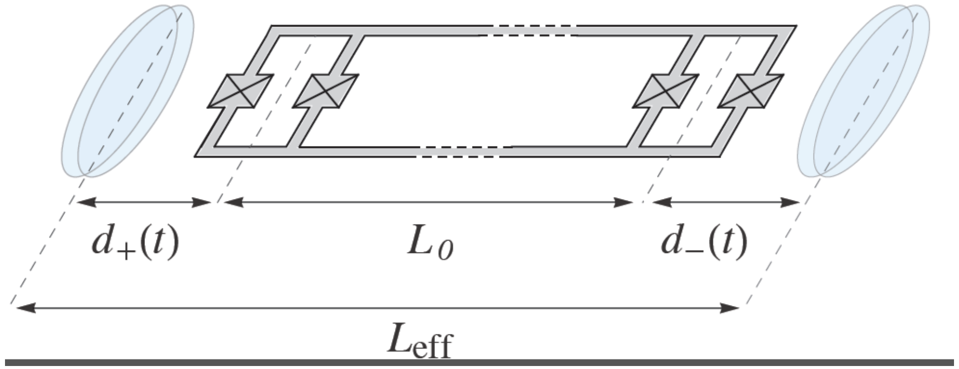

What new did we learn:

Quantum particle creation makes clock tick slower

Precision of quantised light clocks in a Schwarzschild spacetime

Tupac Bravo,[1,*] Dennis Rätzel,[2,†] David Edward Bruschi,[3,4,1,‡] and Ivette Fuentes[5,§]

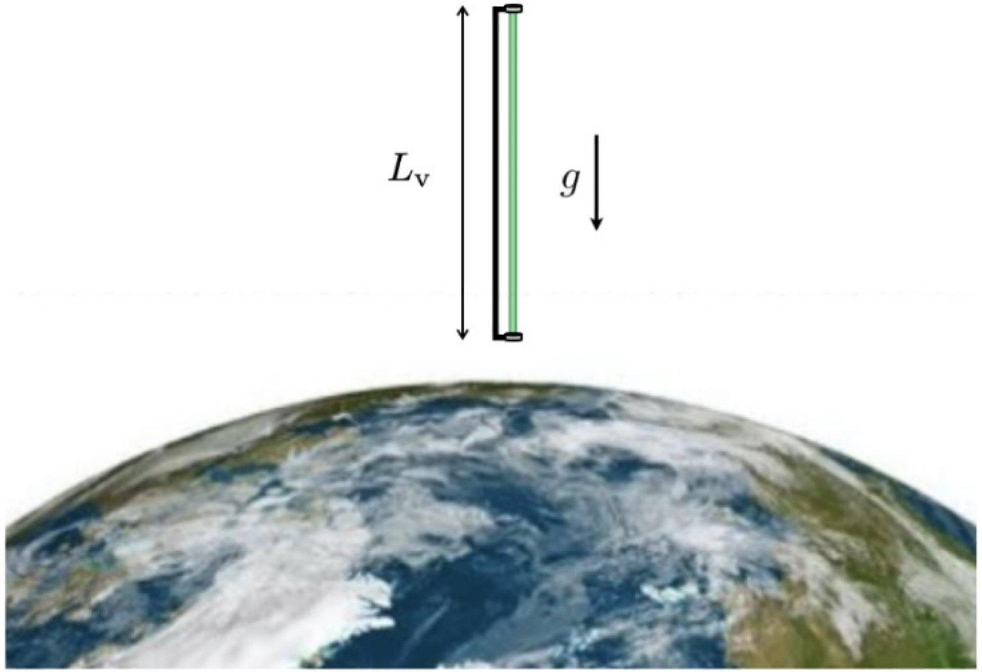

FIG. 1. Vertical light clock in the gravitational field of the Earth. The mirrors are held together by a $L_v = 20cm$ rigid rod.

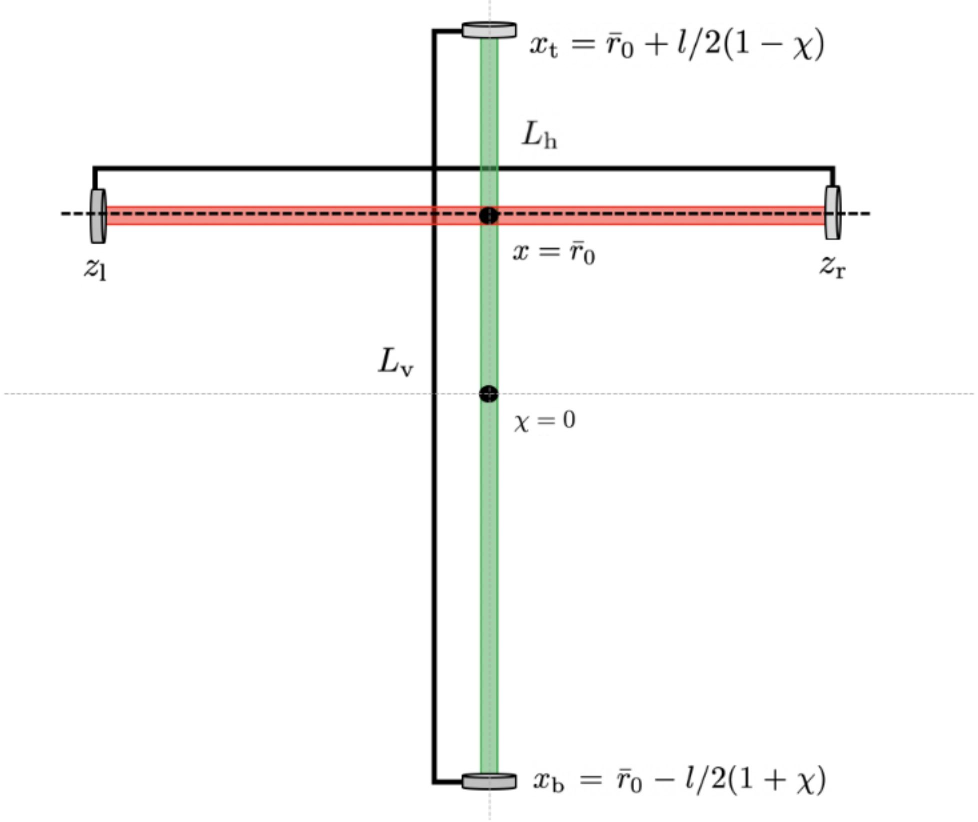

FIG. 4. The horizontal and vertical cavities intersect at $x = \bar{r}_0$. This figure shows where the mirrors are located.

General Relativity and Quantum Cosmology

[Submitted on 16 Apr 2022]

Gravitational time dilation in extended quantum systems: the case of light clocks in Schwarzschild spacetime

Tupac Bravo, Dennis Rätzel, Ivette Fuentes

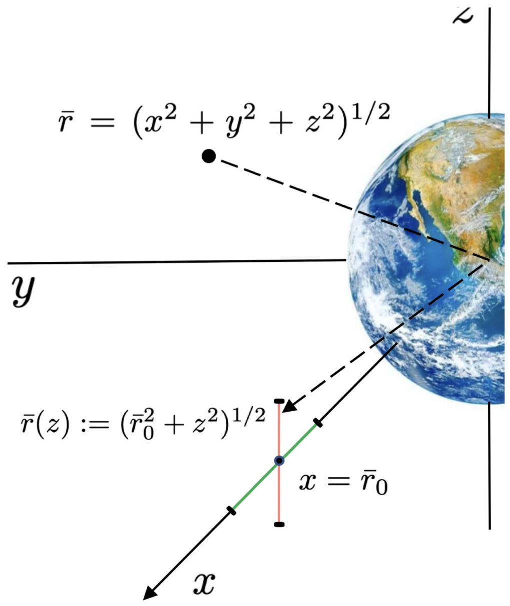

FIG. 1. Coordinate system used to quantize the field in horizontal (red) and vertical (green) cavities.

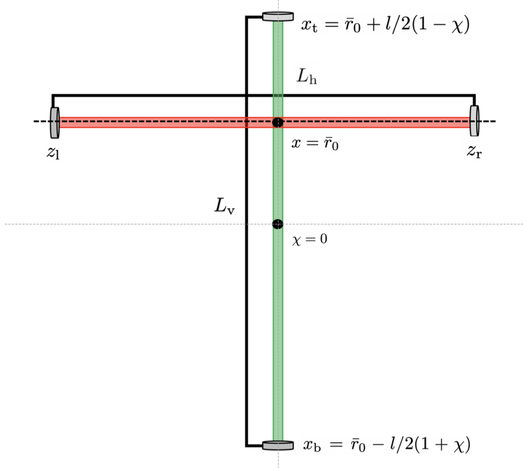

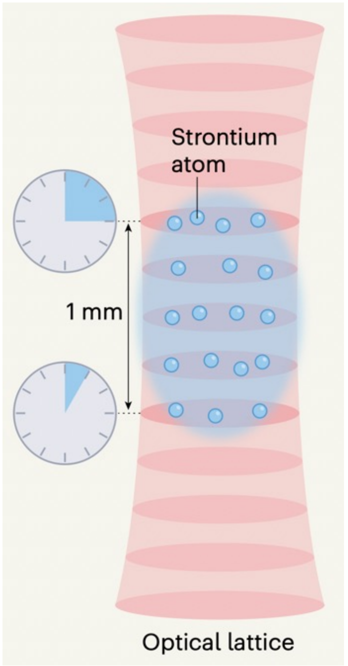

And for quantum clocks with squeezed vacuum input states

$$\Delta_{\mathrm{h},k}(\tau_0) = \frac{1}{2\sqrt{\mathcal{M}}} \frac{1}{\sqrt{N_p(N_p+1)}} \frac{L}{\pi\, c\, k}$$

$$\Delta_{\mathrm{v},k}(\tau_0) = \Delta_{\mathrm{h},k}(\tau_0)\left(1 + \frac{r_\mathrm{S} L}{4\bar{r}_0^2}\chi\right)$$

$$\boldsymbol{g} = \boldsymbol{\eta} + \frac{r_\mathrm{S}}{\bar{r}}\,\mathbb{1} + \frac{r_\mathrm{S}^2}{2\bar{r}^2}\mathrm{diag}\left(-1, \frac{3}{4}, \frac{3}{4}, \frac{3}{4}\right)$$

Clock made of atoms in a trap

Notion of time?

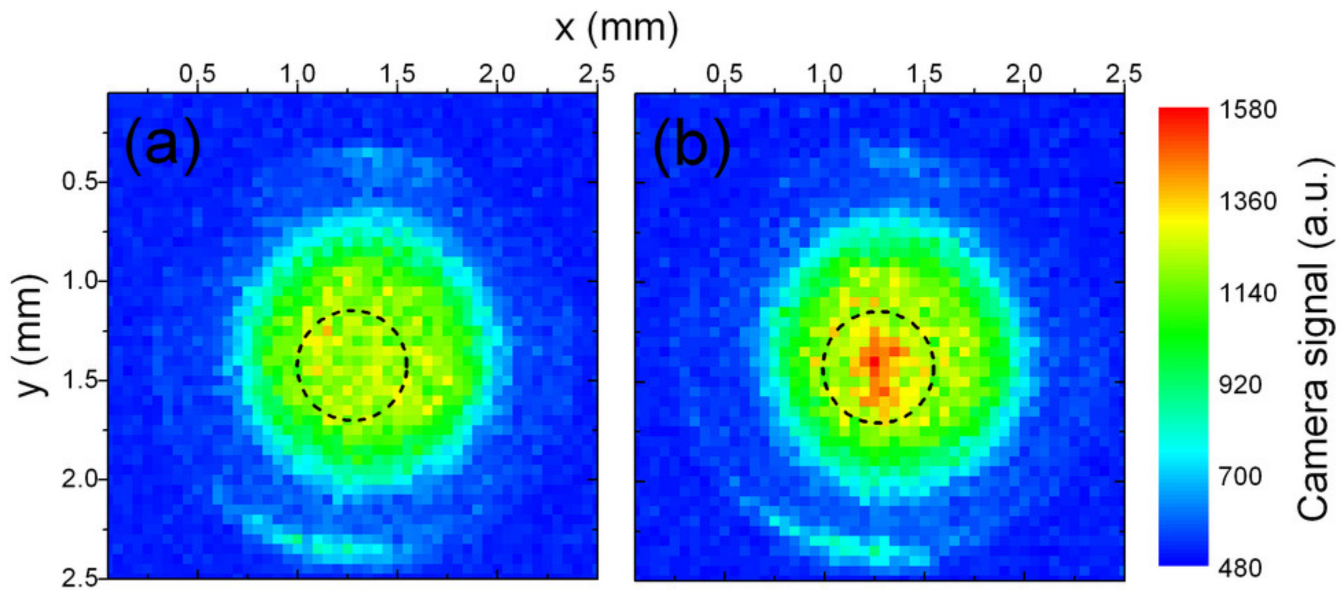

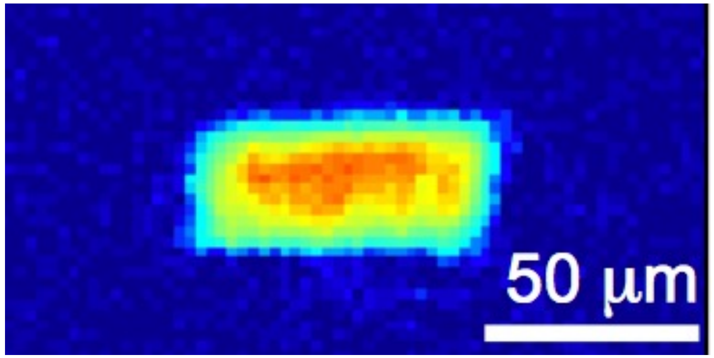

Use collective modes of vibration

Testing gravitational induced collapse

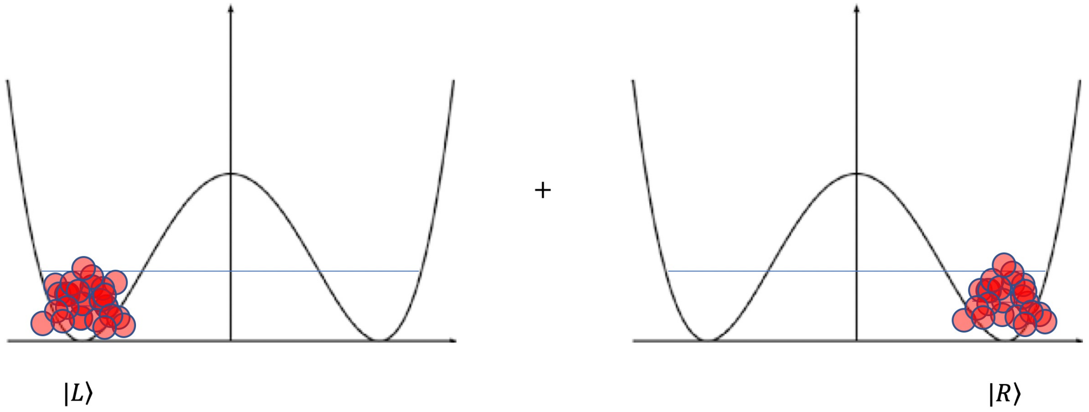

Large mass experiments

Spatial superpositions in a double-well potential

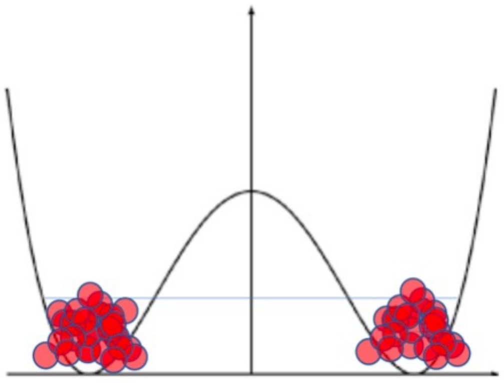

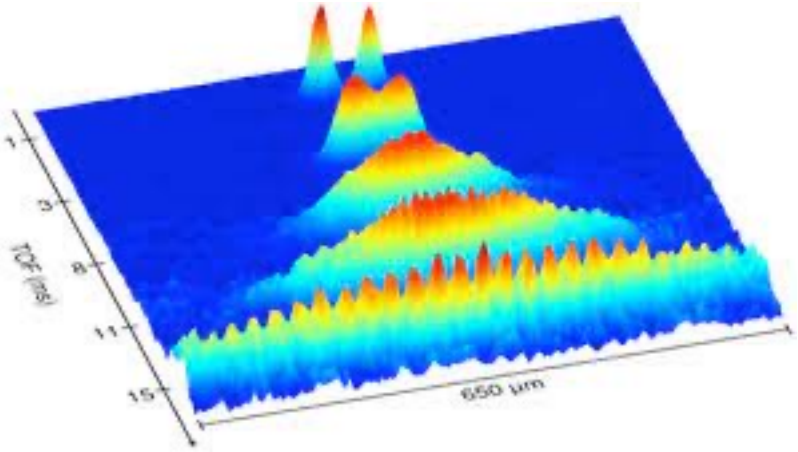

Schrödinger Cat state

$$|\psi\rangle = \frac{1}{\sqrt{2}}(|N_L 0_R\rangle + |0_L N_R\rangle)$$

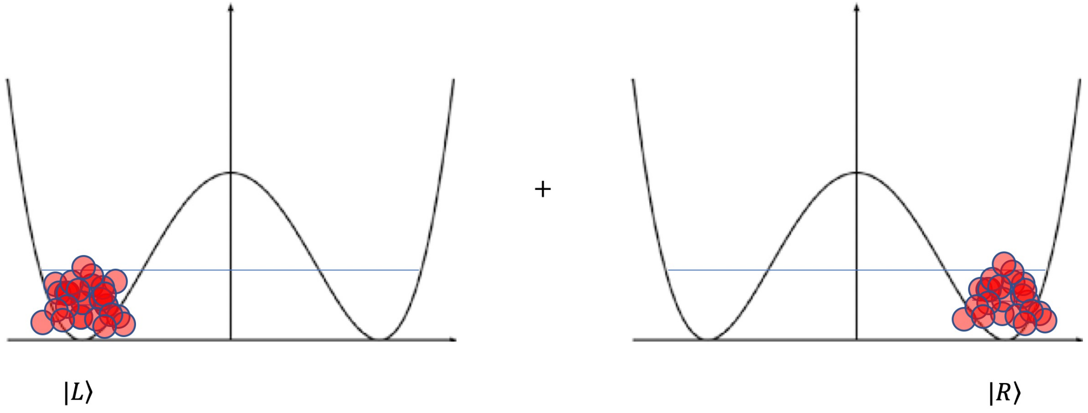

Test Penrose's gravitational induced collapse

Decoherence time must be longer than the collapse time

$$\tau \sim \frac{\hbar}{E_G} \qquad E_G = \frac{13 G m^2 N^2}{14 R}.$$

Non-uniform spherical just touching

Gravitational self-energy

For a uniform sphere

$$E_G = \begin{cases} \frac{6GM^2}{5R}\left(\frac{5}{3}\lambda^2 - \frac{5}{4}\lambda^3 + \frac{1}{6}\lambda^5\right) & \text{if } 0 \leq \lambda \leq 1, \\ \frac{6GM^2}{5R}\left(1 - \frac{5}{12\lambda}\right) & \text{if } \lambda \geq 1, \end{cases}$$

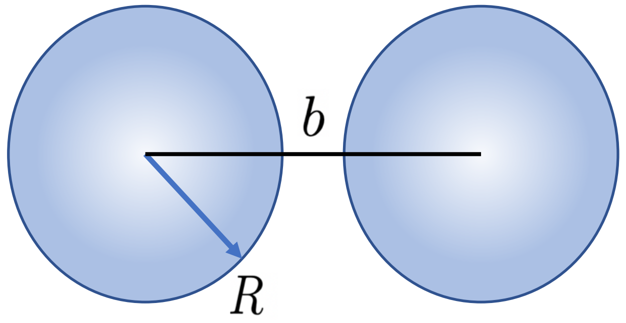

where $\lambda := b/(2R)$

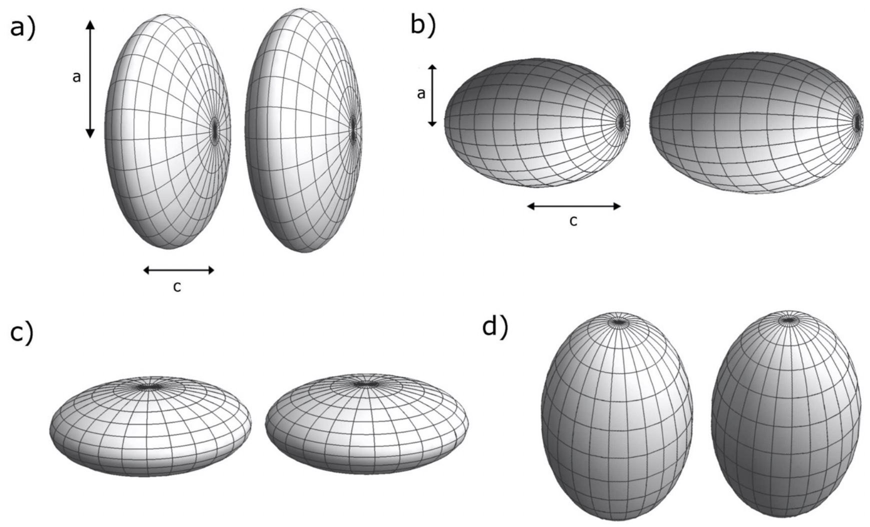

Gravitational collapse depends strongly in the mass geometry: signature

a) and b) can collapse at shorter times depending on the ellipticity

Howl, Penrose & Fuentes, NJP 2019

Decoherence and noise

Howl, Penrose & Fuentes, NJP 2019

- Three-body recombination
- Two-body losses
- Thermal cloud interactions
- Foreign atom interactions
- Decoherence from the trapping potential

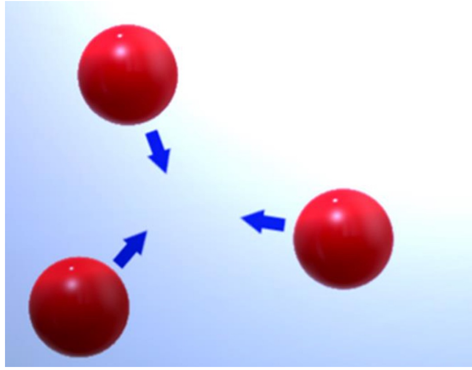

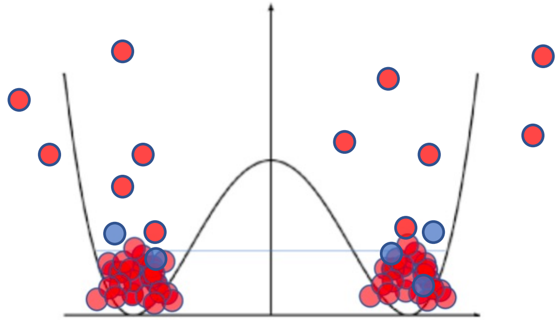

Advantage: atom-atom interactions can be controlled in a BEC

It would be convenient to supressed them after the superposition has been created.

$\gamma = 1/(8\pi)$ A ^{133}Cs BEC with 4x10^9 atoms and R=1 μm would collapse in approximately 2 seconds

$\gamma = 8\pi$ $\quad 2\,\mathrm{s}$ would occur when $N \approx 10^9$ and $R = 0.1\,\mathrm{mm}$ or $N \approx 10^8$ and $R = 1\,\mu\mathrm{m}$.

Confidential: shaking of the building

- Work in progress with Roger, Richard and Devang

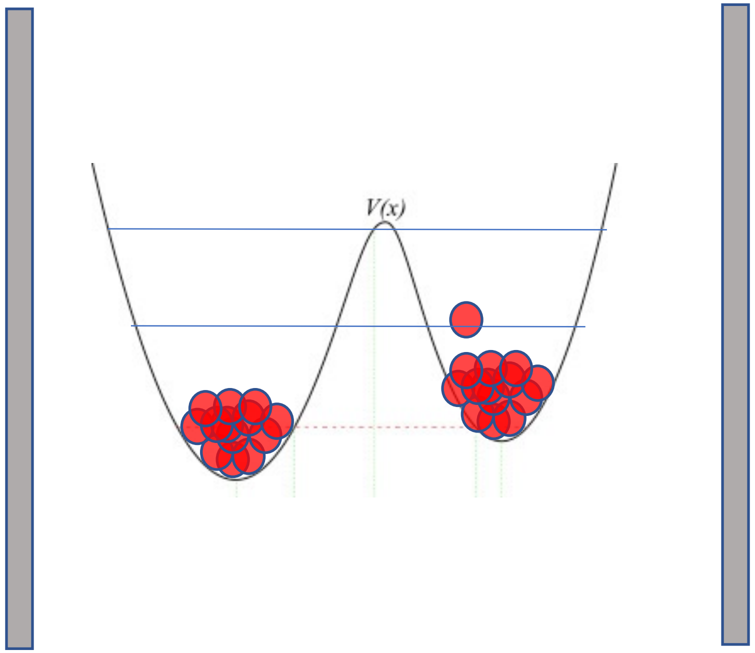

$$\Delta E_G \Delta t = \frac{\hbar}{2}$$

So far, the community has worked on making the gravitational self-energy larger by increasing the mass to get times that are short enough to see collapse. For this N $> 10^9$

For much smaller masses collapse times are very long. We propose to measure a very small energy uncertainty due to gravity: shaking of the building

A very small energy difference between wells can excite and atom to the next energy level. Experiments can detect single atoms in a higher state!

Other BEC states

- Work in progress with Penrose & Westbrook

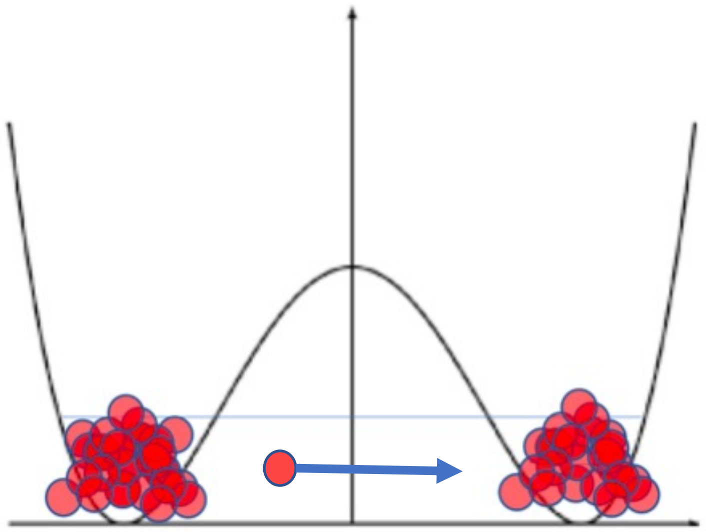

In a BEC atoms are not bound together and can tunnel between left and right wells.

We are studying gravitational self-energy for a variety of BEC quantum states

Gravitational self-energy for spheroidals

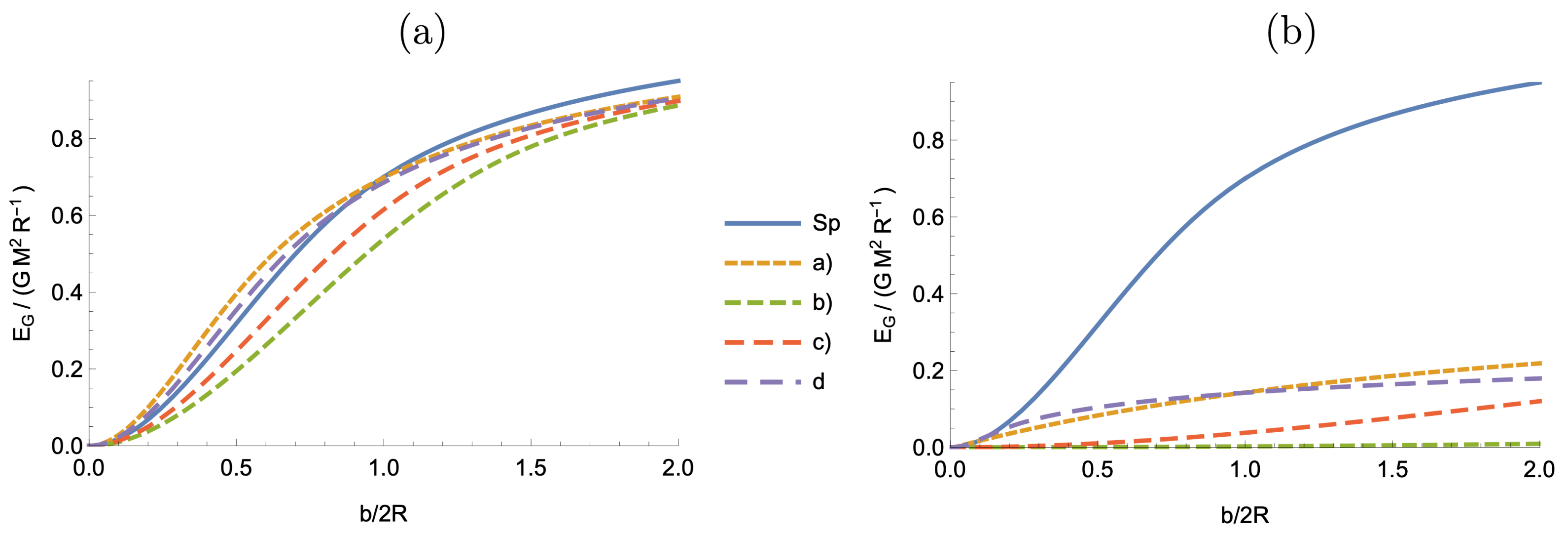

Figure 4. Both plots are of the gravitational self-energy of the difference between displaced uniform spherical and spheroidal mass distributions, E_G, against $b/(2R)$, where R is the radius of the sphere and b is the distance between the centres of the states. All mass distributions have the same total mass and volume. The solid line is for the spherical case, and the various dashed and dotted lines are for the a), b), c) and d) spheroidal configurations illustrated in Figure 3. The left plot is for $\epsilon = 0.5$ (ellipticity $e = 0.87$), and the right plot is for $\epsilon = 0.01$ (ellipticity $e = 0.99995$).

Howl, Penrose, Fuentes, NJP 2019

BEC geometries and density

BEC densities are not uniform
quadratic and Gaussian densities

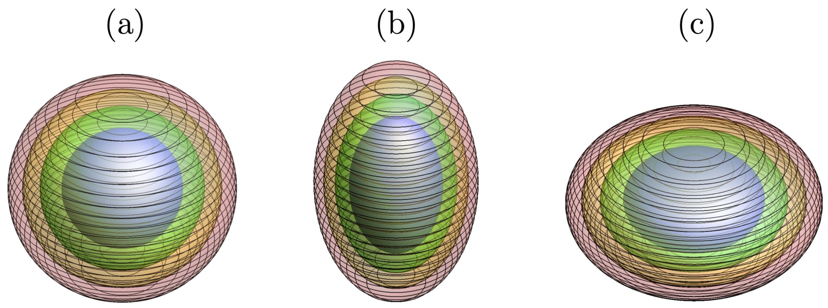

Result: non-uniform densities
produce shorter collapse times

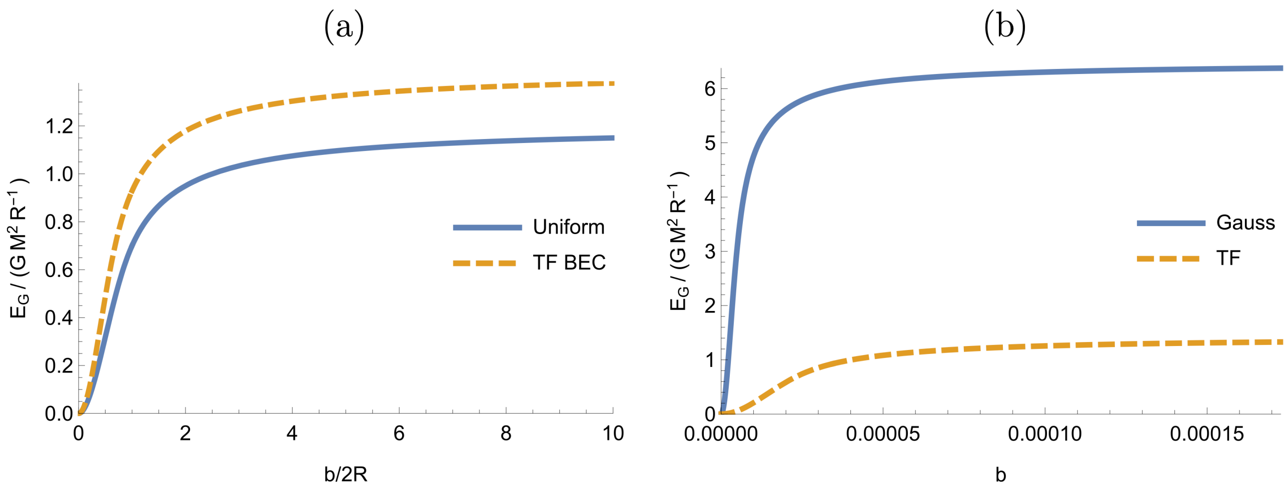

Figure 7. On the left is the gravitational self-energy of the difference between displaced spherical BECs (in the TF approximation) and displaced uniform spheres, $E_G/(GM^2R^{-1})$, against $b/(2R)$ where R is the radius of the spheres, M is their mass and b is the distance between the centres of the sphere states. On the right is $E_G/(GM^2R^{-1})$ against b of spherical ^{133}Cs BECs in the TF and Gaussian approximations with 10^6 atoms, the same trapping frequency $\omega_0 = 100\,\mathrm{Hz}$, and with the standard scattering length in the former regime, but with zero scattering in the latter so that we have an ideal BEC in that case.

Howl, Penrose, Fuentes, NJP 2019

Using Quantum technologies we hope to understand better physics at the interplay of quantum and gravity.